Supporting Information

# Peptide Amphiphile Mediated Co-assembly for Nanoplasmonic Sensing

Zhicheng Jin,[a,†] Yi Li,[a,†] Ke Li,[b,c,†] Jiajing Zhou,[a] Justin Yeung,[d] Chuxuan Ling,[a] Wonjun Yim,[e] Tengyu He,[e] Yong Cheng,[a] Ming Xu,[a] Matthew N. Creyer,[a] Yu-Ci Chang,[e] Pavla Fajtová[f], Maurice Retout,[a] Baiyan Qi,[e] Shuzhou Li,[c] Anthony J. O'Donoghue,[f] and Jesse V. Jokerst[a,e,g*]

[a]Department of NanoEngineering, University of California, San Diego, La Jolla, CA 92093, United States
[b]Institute of Materials Research and Engineering, Agency for Science, Technology and Research, Singapore 138634
[c]School of Materials Science and Engineering, Nanyang Technological University, Singapore 639798
[d]Department of Bioengineering, University of California San Diego, La Jolla, CA 92093, United States
[e]Materials Science and Engineering Program, University of California, San Diego, La Jolla, CA 92093, United States
[f]Skaggs School of Pharmacy and Pharmaceutical Sciences, University of California, San Diego, La Jolla, CA 92093, United States
[g]Department of Radiology, University of California, San Diego, La Jolla, CA 92093, United States

***Corresponding author's email: jjokerst@ucsd.edu (J.V.J.)**

Table of Content

## 1. Materials

Sodium citrate tribasic dihydrate (>99%), gold(III) chloride trihydrate ($HAuCl_4 \cdot 3H_2O$, >99.9%), sodium dodecyl sulfate (SDS, >99%), Trizma® base (>99.9%), Trizma® hydrochloride (>90%), DL-dithiothreitol (DTT, >99%), trifluoroacetic acid (TFA, HPLC grade, >99%), TFA (ReagentPlus®, 99%), Thioflavin T (ThT), epigallocatechin gallate (EGCG, 95%), 2,2′-(ethylenedioxy)diethanethiol (EDDET, 95%), and piperidine (ReagentPlus®, 99%) were purchased from Sigma Aldrich (St Louis, MO). Trypsin (Tp), thrombin (Tb), hemoglobin (Hgb), albumin from bovine serum (BSA), and neuraminidase (or sialidase, 1 U) were also purchased from Sigma Aldrich. Sodium diphenylphosphinobenzene-3-sulfonate (DPPS, >90%), thioanisole (>99%), N,N-diisopropylethylamine (DIPEA, >99%), and triisopropylsilane (TIPS, >98%) were purchased from Tokyo Chemical Industry Co., Ltd. (TCI). Polyethylene glycol 2,000 ($PEG_{2000}$) was from Alfa Aesar (Haverhill, MA). Sodium chloride (certified ACS), urea (certified ACS), and hydrochloric acid (certified ACS plus) were purchased from Fisher Chemical (Waltham, MA). Uranyl acetate solution 2% was from Fisher Scientific (Hampton, NH). Fmoc-protected amino acids, hexafluorophosphate benzotriazole tetramethyl uronium (HBTU), and Fmoc-Rink amide MBHA resin (0.67 mmol/g, 100-150 mesh) were purchased from AAPPTec, LLC (Louisville, KY). Inhibitor GC376 (507.53 g/mol) was purchased from Selleckchem. 5(6)-TAMRA maleimide was from AAT Bioquest (Sunnyvale, CA). Cy3-maleimide and Cy5.5-NHS (no sulfonate) were from Lumiprobe Corp. (Hunt Valley, MD). The pooled whole human saliva and α-amylase (400 U/mL) were purchased from Lee Biosolutions, Inc. (Maryland Heights, MO). The exhaled breath condensation (EBC) was collected from a healthy volunteer (COVID-negative) using a lab condensate tube or a Rtube set-up (from Respiratory Research, Inc.) with an IRB-approved protocol. The recombinant SARS-CoV-2 main protease ($M^{pro}$) was expressed using the $M^{pro}$ plasmid provided by Prof. Rolf Hilgenfeld, University of Lübeck, Germany and purified as previously described.[1] The purified $M^{pro}$ was stored at −80 °C in 20 mM Tris-HCl, pH 8.0, 150 mM NaCl, 1 mM DTT, 5% glycerol. Organic solvents including N,N-dimethylformamide (DMF, sequencing grade), acetonitrile (ACN, HPLC grade), ethyl ether (certified ACS), methylene chloride (DCM, certified ACS), and dimethyl sulfoxide (DMSO, certified ACS) were also from Fisher Scientific (Hampton, NH). Ultrapure water (18 MΩ·cm) was obtained from a Milli-Q Academic water purification system (Millipore Corp., Billerica, MA). TEM grids (formvar/carbon 300 mesh Cu) were purchased from Ted Pella (Redding, CA). 10-mL Disposable reaction vessel and the pressure caps for peptide-resin cleavage were purchased

from Torviq Inc. (Tucson, AZ). The automation compatible syringe filters (hydrophilic PTFE, 0.45 μm) were from MilliporeSigma (St. Louis, MO). Glassware and stir bars were cleaned with aqua regia ($HCl:HNO_3$=3:1 by volume) and boiling DI water before use.

## 2. Instrumentations and Characterizations

***2.1 Peptide synthesis.*** Peptides were chain assembled by Fmoc-SPPS (solid-phase peptide synthesis) on Rink-amide-MBHA-resin (0.67 mmol/g, 200 mg) using an automated Eclipse™ peptide synthesizer (AAPPTec, Louisville, KY). Amino acid couplings were performed under the protection of nitrogen with 0.2 M Fmoc-amino acid (5 *equiv.*) in 3 mL DMF, 0.2 M HBTU in DMF (5 *equiv.*) in 3 mL DMF, 0.3 M DIPEA (7.5 *equiv.*) in 3 mL DMF, and 20% (v/v) piperidine in 2×4 mL DMF for each cycle. The number of coupling cycles was based on the sequence analysis software tool (AAPPTec). The resulting peptides on the resin were transferred into a syringe filter (Torviq Inc.), washed with five rounds of DCM (2 mL each), and dried under vacuum. The peptides were then cleaved from the resin using a cleavage cocktail (3 mL) that contained TFA (82.5%), EDDET (2.5%), phenol (5%), thioanisole (5%), and $H_2O$ (5%). Resins were treated with the cleavage cocktail for 2-3 h with gentle shaking. After cleavage, the resin was filtered and the filtrate containing the crude peptides was precipitated/washed with three rounds of cold ether (10 mL, −20 °C), suspended in 50% ACN/$H_2O$ (10 mL, *v/v*), and lyophilized in a FreeZone Plus 2.5 freeze dry system (Labconco Corp., Kansas, MO). Peptides were purified by the C18 reversed phase HPLC (Shimadzu LC-40), confirmed by the ESI-MS, aliquoted ($\varepsilon_{205}$ ~74.6 $mL \cdot mg^{-1}\ cm^{-1}$) using a NanoDrop™ One UV-vis spectrophotometer (Thermo Fisher Scientific), and stored in dry conditions at −20 °C for further use; see below for the work-up steps.

Peptide purification was carried out using a Shimadzu LC-40 HPLC system equipped with a LC-40D solvent delivery module, photodiode array detector SPD-M40, and degassing unit DGU-403. The crude sample was dissolved in an acetonitrile/$H_2O$ mixture (1:1, v/v) with the injection volume of 2 mL, applied on a Zorbax 300 BS, C18 column (5 μm, 9.4×250 mm) from Agilent (Santa Clara, CA), and eluted at a flow rate of 1.5 mL/min over a 40 min linear gradient from 10% to 95% of acetonitrile in water (with 0.05% TFA, HPLC grade). Preparative injections were monitored at 190, 220, and 254 nm. Fractions containing the pure peptide as confirmed by electrospray ionization mass spectroscopy were lyophilized and aliquoted (see below). All peptides were purified by HPLC to reach a purity of at least 90%.

Peptide synthesis and cleavage was confirmed using electrospray ionization mass

spectrometry (ESI-MS, positive ion mode) *via* the Micromass Quattro Ultima mass spectrometer in the Molecular MS Facility (MMSF). ESI-MS samples were prepared in a MeOH/$H_2O$ mixture (1:1, v/v).

Peptide concentration was determined using a NanoDrop™ One UV-vis spectrophotometer (Thermo Fisher Scientific, Waltham, MA): The 31-method was applied for peptides lacking tryptophan (W) and tyrosine (Y) residues otherwise the Scopes method was used. The absorption coefficient of $\varepsilon_{205}$ ~74.6 $mL \cdot mg^{-1} cm^{-1}$ was used (note that DMSO or acetonitrile contributes absorbance signal at 205 nm; thus, water or alcohol is used as the blank).[2]

***2.2 Proteolysis of peptide.*** A peptide solution (500 μL, 1 mg/mL, DMSO <1% v/v) in phosphate buffer (10 mM, pH 8.0) was incubated with the $M^{pro}$ at a molar ratio of 3000:1 (substrate: enzyme) at 37 °C for 18 h to make a peptide fragment solution.

First, to confirm the $M^{pro}$ cleavage site, the above mixture was applied on a Shim-pack GIS, C18, analytical column (5 μm, 4.6×100 mm) from Agilent and eluted at a flow rate of 1 mL/min with a 40-minute gradient from 10% to 95% acetonitrile in DI water (with 0.05% TFA, HPLC grade). Preparative injections were monitored at 190, 220, and 254 nm. All fractions were collected, and the eluent's molecular weight was determined using the ESI mass spectrometer. Second, for majority of the SLPs the HPLC pattern (**Figure S2**) also confirmed a near complete substrate depletion under the conditions of substrate-enzyme molar ratio of 3000:1 at 37 °C for 18 h in PB (10 mM, pH 8.0). In addition, a fluorogenic peptide Cy3-$D_3F_2C_1$-Cy5.5 (see preparation protocol below) was incubated with $M^{pro}$ under the same assay conditions, and the reaction at 3 h (partial depletion) and 18 h (complete depletion) were monitored over HPLC for tracking the degree of substrate digestion by $M^{pro}$ (**Figure S4**).

To characterize the secondary structure formation after proteolysis, the fragmented peptide solutions were aged for 48 h at room temperature, and then their Fourier transform infrared (FTIR) data were collected using a Bruker Tensor II FTIR spectrophotometer by drying the corresponding solution on the optical window.

To study the peptide self-assembly kinetic, a peptide solution (100 μL, 600 μM, DMSO <1% v/v) in phosphate buffer (10 mM, pH 8.0) was loaded in dynamic light scattering (DLS) cuvette, swiftly mixed with $M^{pro}$ (2 μL, 38 μM), capped, and incubated in a 37 °C water bath. The hydrodynamic size of the mixture was measured in a Zetasizer Nano ZS90 (Malvern Panalytical, Inc.) over 1 h with 10 min interval time. Measurements were done in duplicate.

Note that the refractive index for peptide content is set to 1.45.

The morphology of peptide assembly was verified under transmission electron microscopy (TEM): 4 μL of the peptide fragment suspension was dropped cast onto a plasma pre-cleaned carbon coated copper grid (300 mesh, Ted Pella). After drying, the grid was then stained with 10 μL of 2% (w/v) uranyl acetate for 2.5 min and blotted on a Kimwipe. The staining process was repeated once as above. Then 10 μL of DI water was applied to wash the salt residues and the grid was dried at 37°C for TEM measurement (a JEOL 1200 EX II operated at 80 kV). The method of molecular dynamics simulation on the peptide fragment self-assembly is provided in the main text, Experimental Section.

***2.3 Fluorogenic peptide synthesis.*** An Cy3/Cy5.5 FRET pair was chosen to make the fluorogenic substrate. First, in a scintillation vial equipped with a stir bar an aqueous solution of $D_3F_2C_1$ peptide (7.8 mM, in 200 μL PB, pH 8.0) was mixed with TCEP (62.4 mM, in 50 μL PB, pH 8.0) for 30 min. Then, Cy3-maleimide (3.9 mM, in 200 μL DMSO) was added to the above mixture, the reaction pH was adjusted to 8.0 by NaOH (1 M) and stirred for 1 h protected from light. The reaction was quenched and dried in a speed vacuum system at 60 °C for 3 to 4 h.

The crude $D_3F_2C_1$-Cy3 pellet was dissolved in an acetonitrile/$H_2O$ mixture (1:1, v/v) with the injection volume of 1 mL, applied on a SPIRIT PROTEIN 300, C4 column (5 μm, 1×25 cm) from AAPPTec, LLC (Louisville, KY), and eluted at a flow rate of 3.0 mL/min over a 60 min linear gradient from 10% to 90% of acetonitrile in water (with 0.05% TFA, HPLC grade). Preparative injections were monitored at 220 and 550 nm. The fraction containing the pure peptide-dye as confirmed by ESI-MS (**Figure S3**) was aliquoted (*i.e.*, $\varepsilon = 1.5 \times 10^5$ $M^{-1}$ $cm^{-1}$ at $Abs._{555\ nm}$), dried by a speed vacuum system, and stored at -20 °C covered with aluminum foil (with a yield of ~80%).

Second, in a scintillation vial equipped with a stir bar, the $D_3F_2C_1$-Cy3 (1.77 mM, in 150 μL DMSO) was mixed with triethylamine (1.5 μL, in 400 μL DMSO) and Cy5.5-NHS (32.5 mM, in 17 μL DMSO) for 1 h protected from light. The reaction was quenched and dried in a speed vacuum system at 60 °C for overnight.

The crude Cy5.5-$D_3F_2C_1$-Cy3 pellet was dissolved in an acetonitrile/$H_2O$ mixture (1:1, v/v) with an injection volume of 1 mL. This was then applied on a spirit protein 300, C4 column (5 μm, 1×25 cm) from AAPPTec, LLC (Louisville, KY), and eluted at a flow rate of 3.0 mL/min over a 60 min linear gradient from 40% to 90% of acetonitrile in water (with 0.05%

TFA, HPLC grade). Preparative injections were monitored at 220, 550, and 650 nm. Fractions containing the pure peptide-dye as confirmed by ESI-MS (**Figure S3**) were aliquoted (*i.e.*, $\varepsilon$ = $1.5 \times 10^5$ $M^{-1}$ $cm^{-1}$ at $Abs._{555\ nm}$ or $\varepsilon = 1.98 \times 10^5$ $M^{-1}$ $cm^{-1}$ at $Abs._{685\ nm}$), dried by a speed vacuum system, and stored at -20 °C covered with aluminum foil (with a yield of ~60%).

The synthetic protocol of Cy3-GTSAVLQ↓SGFK-Cy5.5 substrate can be found in our previous literature.[3]

***2.4 Gold nanoparticle.*** The citrate-AuNPs (~13 nm diameter, TEM) were prepared using the Turkevich method by rapidly injecting an aqueous solution of sodium citrate tribasic dihydrate (150 mg, 5 mL) into an aqueous solution of $HAuCl_4 \cdot 3H_2O$ (45 mg, 300 mL) under boiling conditions and vigorous stirring. The reaction mixture was left boiling while stirring for another 20 min and then cooled to room temperature. The deep red dispersion was then purified by applying one round of centrifugation at 18,000 *g* for 30 min and the supernatant was discarded. The resulting pellet of citrate-AuNPs was redispersed in DI water by sonication and stored at ambient conditions ($\varepsilon_{520}=4.0\times10^8$ $M^{-1}$ $cm^{-1}$). To prepare the DPPS-AuNPs, the DPPS solution (200 mg in phosphate buffer of 10 mM, PH 8.0) was added to a flask containing citrate-AuNPs (200 mL, 3.4 nM) equipped with a stir bar. The mixture was stirred at 1,600 RPM for 18 h at room temperature. The resulting gold colloids were split into 50 mL of each and precipitated twice by centrifugation at 18,000 *g* for 40 min. The supernatant was discarded, and the pellet was redispersed in DI water, passed through a syringe filter (0.45μm, hydrophilic PTFE), and stored at 4 °C for further use.

The optical absorption measurements were collected using a hybrid multi-mode microplate reader (Synergy™ H1 model, BioTek Instruments, Inc.) in a 96-well plate. The DLS and zeta potential (ζ) measurements were carried out using a compact Zetasizer Nano ZS90 (Malvern Panalytical, Inc.). Transmission electron microscopy (TEM) images of the Au colloids were acquired using a JEOL 1200 EX II operated at 80 kV. The TEM grids were prepared by drop casting aqueous samples (4 μL) followed by natural drying. The size analysis was performed using a MANTA ViewSizer 3000 instrument (Horiba Scientific, Irvine, CA) with following settings: 15 ms exposure, 30 dB gain, 60 mW blue laser (445 nm) power, 12 mW green laser (520 nm) power, and 8 mW red laser (635 nm) power, 25 °C, the applied $c_{\text{final}}{}_{\text{NPs}}$ ranges from 0.2 to 0.6 nM. The ligands on the gold surfaces were identified using a Bruker Tensor II FT-IR spectrophotometer through lay-by-layer drying the nanoparticle dispersion on the detection window.

***2.5 Agarose gel electrophoresis.*** Gel electrophoresis measurements were applied side-by-side to the AuNPs modified with different surface molecules. They were conducted on a 0.7% (w/v) agarose gel prepared in 100 mL of TBE buffer (1× strength, 89 mM tris, 89 mM boric acid, 1 mM EDTA). The aliquots (40 μL) of the AuNPs (~20 nM) were mixed with 10 μL of glycerol, homogenized then loaded into the gel wells, and run at 6.5 V/cm for 30 min. The white-light images were taken by a smartphone in a lightbox.

**3. Enzyme Kinetic and Specificity Constant ($k_{cat}/K_M$)**

The kinetic model of an enzyme is largely developed by Michaelis and Menten[4] and Henri[5], with significant improvements by Briggs-Haldane[6]. In the simplest scheme, the enzyme and substrate reversibly form an enzyme-substrate complex, followed by dissociation of the intermediate complex to produce the product with free enzyme, which is given as

$$E + S \underset{k_{off}}{\overset{k_{on}}{\rightleftharpoons}} ES \underset{k_{-cat}}{\overset{k_{cat}}{\rightleftharpoons}} E + P \tag{S1}$$

where $k_{on}$, $k_{off}$, $k_{cat}$, and $k_{-cat}$ are rate constants. The relationship between the initial velocity of product formation ($\upsilon$) and the substrate concentration ($[S]_0$) is known as the classical Michaelis-Menten (MM) equation

$$\upsilon = \frac{\upsilon_{max} \cdot [S]_0}{K_M + [S]_0} \tag{S2}$$

where $\upsilon_{max}$ is the maximum velocity and $K_M$ is the MM constant; the subscript 0 denotes the *total* concentration. When $[S]_0 = K_M$, the initial velocity reaches ½ $\upsilon_{max}$. Because the $k_{cat}$ is the rate limiting step in enzymatic reactions, therefore

$$\upsilon \equiv \frac{d[P]}{dt} = k_{cat}[ES] - k_{-cat}[E][P] \tag{S3}$$

Dissociating the ES complex is usually treated as an irreversible process due to the low affinity of enzyme to product, and thus $k_{-cat}$ is negligible:

$$\upsilon \approx k_{cat}[ES] \; or \; \upsilon_{max} = k_{cat}[E]_0 \tag{S4}$$

Experimentally, in a 96-well plate the fluorogenic substrate was diluted in phosphate buffer (10 mM, pH 8.0) to reach a final $[S]_0$ of 1.0, 2.7, 7.4, 20.2, and 55.0 nM (*i.e.*, with respect to a 60 μL volume). The $M^{pro}$ (active $[E]_0$ = 200 nM with respect to a 60 μL volume) was then

added to each well and the total volume was brought to 60 μL using PB. Next, the plate was incubated at 37 °C in a hybrid multi-mode microplate reader with 3 s of shaking before each cycle of reading, and the photoluminescence intensity (PL at 570 nm for Cy3) was recorded over 12 h with 1 min intervals between each cycle. Measurements were done in triplicates. Triplicate PL values at 30 min readout time were averaged and plotted against substrate concentrations; error bars represent the standard error of the means. The $\Delta PL = PL_{30\ min} - PL_{0\ min}$ was then correlated to product concentration using a standard curve: ΔPL of Cy3 versus [$D_3F_2C_1$-Cy3]. Data were then fitted to the above Michaelis-Menten equation (**Figure S3**).

## 4. Molecular Dynamics (MD) Simulation

***4.1 Aggregation propensity of peptide segments.*** The initial structures of SGGFPC, SGFFPC, SGFFPFFPC, and DDDTSAVLQSGFFPC were built using Avogadro software. Note that these simulations all used an amidated C-terminus; see chemical structure in **Figure S6**. Four cubic simulation boxes were constructed with side lengths of 100 Angstroms (or 10 nm). For each type of the peptide, 20 copies were packed into the cubic simulation box using a random packing algorithm in Packmol. All simulation boxes were solvated with water molecules. In the case of DDDTSAVLQSGFFPC peptide, the $Na^+$ counterion was introduced to balance the charge. The water model used in these simulations was TIP3P, and the SHAKE algorithm was used to constrain the bond lengths and bond angles in the water molecules. The Amber force field described the intra- and inter-molecular interactions of the peptide molecules. After random packing, each box was energy minimized and then equilibrated in the NPT ensemble for 5 ns at 298 K and 1 atm following a 40-ns production run at the same ensemble. All simulations were performed within the GROMACS software package under periodic boundary conditions with a 1-fs time step using Ewald, specifically PEM, to account for long-range electrostatics. The partial charges on the atomic sites of all the molecules for use in the MD simulations were determined using the RESP2 approach[7] with Multiwfn software. The electronic structure calculations were performed at the B3LYP/def2TZVP level using the Gaussian 09 software[8].

The results of MD simulation were discussed below. We performed simulation for peptide behavior of intact $D_3F_2C_1$ and its fragment (*i.e.*, SGFFPC) in water to investigate the aggregation propensity of SLP before and after proteolysis.[9] We also simulated another two fragments (*i.e.*, SGGFPC and SGFFPFFPC) to understand the effect of the number of Phe residues on the assembly kinetic at molecular level. Four simulation boxes (10 × 10 × 10 nm)

were constructed and randomly filled with 20 copies of each peptide and water molecule (*i.e.*, scattered red dot in **Figure S6e-h**); the 40-ns production run in these systems was analyzed. According to **Figure S6**, the initial SGFFPC monomer condensed into one large peptide aggregate at 40 ns of simulation time, whereas the intact $D_3F_2C_1$ (with $Na^+$ counterions) gave rise to limited or no self-assembly. This agrees with the patterns from the above TEM data and supports our hypothesis that the designed SLPs condense to a large supramolecular structure after proteolysis.

We then analyzed non-covalent bond compositions (*e.g.*, H-bonding and aromatic stacking interactions) and solvent-accessible surface area (SASA) of the peptide assemblies in the above four systems. **Figure S6b,c** shows that the number of π-stacking involved in SGGFPC, SGFFPC, SGFFPFFPC, and the intact $D_3F_2C_1$ systems at 40-ns is about 22, 63, 145, and 21, respectively. That is, the SGFFPFFPC aggregates have 2.3- and 6.6-fold more aromatic forces than those of SGFFPC and SGGFPC assemblies, respectively. A close inspection of the time-dependent aromatic interactions in the systems reveals that SGFFPFFPC and SGFFPC rapidly plateau as the simulation proceeded; such interactions in SGGFPC and intact $D_3F_2C_1$ are still far away from equilibrium over simulated time courses. A similar trend was observed in hydrogen bonding in these peptide aggregates. Likewise, **Figure S6d** indicates that the reduced SASA (*i.e.*, $\Delta_{SASA} = SASA_{40ns} - SASA_{0ns}$) in SGFFPFFPC and SGFFPC system is ~2.5-times more than that of SGGFPC and intact $D_3F_2C_1$ at initial 10 ns. This indicates that the peptide assemblies stacked from SGFFPFFPC and SGFFPC exhibit less surface area and therefore are larger in the aggregation dimension compared to the later. Overall, these simulations suggest that the inclusion of more Phe in the peptide sticker favors π−π interactions, which promotes rapid self-assembly and creates large aggregates. This agrees with the notion of assembly kinetics measured by DLS and TEM techniques (**Figure 2**).

***4.2 SGFFPC-based nanofiber.*** Four copies of SGFFPC molecules were packed with water molecules into the cubic simulation box with a side length of 50 Angstroms. The box was energy minimized and then equilibrated in the NPT ensemble for 10 ns at 298 K and 1 atm. After 10 ns equilibrium, the peptides formed a cluster of four peptides. The peptides interact with hydrogen bond and pi-pi interactions. The initial structure of SGFFPC nanofiber consists of 64 SGFFPC molecules and was built by stacking the four-peptide cluster horizontally. The SGFFPC nanofiber was packed in a cuboid simulation box with a length of 400 in *x*-direction 30 in *y*-direction and 30 in *z*-direction. The simulation was energy minimized and then

equilibrated in the NPT ensemble for 20 ns at a temperature of 298 K and 1 atm.

The water model used in these simulations was TIP3P[10], and the SHAKE[11] algorithm was used to constrain the bond lengths and bond angles in the water molecules. The Amber[12] force field was chosen to describe the intra and inter molecular interactions of peptide molecules. All the above simulations were carried out within the GROMACS[13] software package under periodic boundary conditions with a 1 fs time step using Ewald, specifically PME, to account for long-range electrostatics. The partial charges on the atomic sites of all the molecules for use in the MD simulations were determined using the RESP2[14] approach using Multiwfn[15] software. The electronic structure calculations were performed at the B3LYP/def2TZVP level using the Gaussian 09[8] software.

The results of MD simulation show that after 20 ns simulation time, the fibril structure remained tubular structure (**Figure S6**). This is consistent with our experimental observations that the peptide stickers not only have assembly behavior but also condense into ordered and linear structures.

**5. ThT Fluorescence Kinetic Assay**

The peptides were dissolved in phosphate buffer (10 mM, pH 8.0) at a final concentration of 300 μM (DMSO <1% v/v). The peptide solution was then incubated with the $M^{pro}$ at a molar ratio of 3000:1 (substrate : enzyme) at 37 °C for 3 h. The fragmented peptide solutions were aged for 48 h at room temperature with frequent shaking. Aqueous ThT (prepared in PB buffer) was then added to the aged peptide sample to a final concentration of 50 μM ThT and 300 μM peptide.[16] Data were collected in a hybrid multi-mode microplate reader (Synergy™ H1 model, BioTek Instruments, Inc.) in a 96-well plate covered with a SealPlate film (EXCEL Scientific, Inc.) The plate was incubated at 37 °C with 5 s of shaking before each cycle of reading, and data were collected over 1 h with 1 min intervals between each cycle. On excitation at 438 nm, the ThT fluorescence intensity at 485 nm was recorded over time. Measurements were done in triplicate. Note the phosphate buffer only incubated with ThT was used as a control.

**6. FT-IR of Peptide Fragments Assemblies**

Fourier transform infrared (FT-IR) spectrum was applied to study the β-sheet nature of SGFFPC-formed superstructures. Generally, the amide-I absorption (1700 – 1600 $cm^{-1}$) is primarily determined by the assembled backbone conformation and independent of the amino

acid sequence, *e.g.*, the average frequency of β-sheet as the main component is about 1626 and 1613 $cm^{-1}$, while a predominant α-helical conformation presented a mean frequency at 1652 $cm^{-1}$.[17] The measured FT-IR profiles for the intact $D_3F_2C_1$, $S_3F_2C_1$, and $(PAS)_2F_2C_1$ peptide exhibited a broad band ranging from 1660 –1640 $cm^{-1}$, which originates from a combination of 80% C=O stretching, 10% C-N stretching, and 10% C-N bending in the amide bond.[18] In comparison, a sharp peak emerges near 1626 $cm^{-1}$ for the $M^{pro}$-cleaved SLPs (**Figure S8**). Therefore, the IR spectra indicate that peptide assemblies from SGFFPC had a prevailing β-sheet structure with no α-helix content. This is different from the unique helical-like β-sheet formed by the short PFF tripeptide; nonetheless, these results similar to those FF-appended peptides that directly form β-type aggregates without going through α-helical barrels.[19] In contrast, the $D_3F_1C_1$ peptide showed no prominent difference in the FT-IR profiles before and after proteolysis, suggesting limited aggregation of SGGFPC.

**7. Probe Interparticle Interactions**

In a 0.5-mL microtube gold nanoparticle dispersion (100 μL, 3.4 nM) was thoroughly mixed with the corresponding peptide fragment solution (30 μL, 600 μM) until no more color change. The mixture was then mildly centrifuged at 500 *g* for 1 min and the supernatant was discarded. The pellet was then added with the probing solution (100 μL) and sonicated for 10 s, including DI water, $PEG_{2000}$ (10 mM), Triton X-100 (10 mM), HCl (10 mM), NaOH (10 mM), NaCl (10 mM), Urea (1 M), SDS (10 mM), DMSO (100%), DMF (100%), citric acid (10 mM), sodium citrate tribasic (10 mM), and DPPS (10 mM). Ratiometric absorbance data ($Abs_{600}/Abs_{520}$) were collected in a hybrid multi-mode microplate reader (Synergy™ H1 model, BioTek Instruments, Inc.) in a 96-well plate. The negative and positive control use gold nanoparticle only and particle dispersion with peptide fragments, respectively. Data on citrate-AuNPs were presented but the test on DPPS-AuNPs showed the similar trend.

**8. Sensor Dynamic Range (Working Window)**

The intact peptide was dissolved in phosphate buffer (10 mM, pH 8.0, DMSO < 1% *v/v*) for use. The peptide fragments were prepared by incubating the corresponding intact peptide with $M^{pro}$ at a molar ratio of 3000:1 at 37 °C for 3 h. Next, DPPS-AuNPs (100 μL, 3.4 nM) were mixed with the intact or fragmented peptides (20 μL) in a 96-well plate to reach final concentrations of 0, 1, 2, 5, 10, 20, 30, 40, 50, 60, 80, and 100 μM. Data were collected in a hybrid multi-mode microplate reader (Synergy™ H1 model, BioTek Instruments, Inc.). The

plate was incubated at room temperature, with 3 s shaking before each cycle of reading, and ratiometric absorbance data ($Abs_{600}/Abs_{520}$) were recorded over 3 h with 1-min intervals between each cycle. The measurements were done in duplicate. Duplicate ratiometric values at 3 h were averaged and plotted against peptide concentrations, and the standard error of means was represented as error bars. Phosphate buffer only was used as the control.

The dynamic working window for peptide/citrate-AuNPs was obtained following the same protocol as above except that the readout time at 10 min. The mixtures peptide/particles were further diluted to 800 μL with DI water and the hydrodynamic diameter ($D_H$) and zeta potential (ζ) were measured in a Zetasizer Nano ZS90 (Malvern Panalytical, Inc.).

## 9. LoD Measurement

The $M^{pro}$ was spiked into phosphate buffered (10 mM, pH 8.0), EBC (single donor), pooled human saliva (50% dilution), and human plasma (50% dilution) to reach a final $c_{Mpro}$ of 0, 1, 2, 5, 10, 15, 20, 22, 25, 28, 30, 50, 100 nM (*i.e.*, with respect to a 140 μL volume). The intact $D_3F_2C_1$ peptide (20 μL, 700 μM) was then added to the mixtures in microtubes and the total volume was brought to 40 μL using the test media. Next, the above mixtures were flicked, centrifuged, and incubated at 37 °C for 3 h. The reaction was then transferred into a 96-well plate and incubated with DPPS-AuNPs (100 μL, 3.4 nM). The plate was incubated at room temperature in a hybrid multi-mode microplate reader with 3 s of shaking before each cycle of reading, and ratiometric absorbance data ($Abs_{600}/Abs_{520}$) were recorded over 3 h with 1 min intervals between each cycle. Measurements were done in duplicate. Duplicate ratiometric values at 3 h readout time were averaged and plotted against $M^{pro}$ concentrations; error bars represent the standard error of the means. *Remark:* The LoD for the peptide/citrate-AuNPs was determined following the same protocol as above except for the readout time at 10 min. The LoD calculation follows a reported statistical method:[20]

$$\mathrm{LoD_{int.}} = \mathrm{mean_{blank}} + 1.645 * (\mathrm{SD_{blank}}) + 1.645 * \left(\mathrm{SD_{low\ concentration\ sample}}\right) \qquad (S5)$$

## 10. Specificity Test

***10.1 Human subjects.*** This study was approved by the Human Research Protections Program at the University of California, San Diego (project# 202019). Informed written consent from each participant was acquired before testing. The inclusion criteria were as follows: (i) participants had to be 18 y and able to provide consent; and (ii) participants were confirmed to

be COVID-19 negative by standard PCR test.

***10.2 Inhibitor assay for $M^{pro}$.*** The $M^{pro}$ inhibitor (GC376) of desired amount was pre-incubated with the $M^{pro}$ (1.6 μL, 3.8 μM) at molar ratios of 0, 0.05, 0.1, 0.2, 0.4, 0.8, 1.6, 2.5, 5, and 10 at ambient condition for 10 min. Then, the intact $D_3F_2C_1$ peptide was mixed with the inhibited enzyme and the assay volume was brought to 20 μL with phosphate buffer (10 mM, pH 8.0) to reach a final concentration of 300 nM $M^{pro}$ and 600 μM intact peptide. Next, the mixtures were tapped, centrifuged, and incubated at 37 °C for 30 min. After that, the inhibitor assay was transferred into a 96-well plate, incubated with citrate-AuNPs (100 μL, 3.4 nM), and readout the absorbance at 600 and 520 nm in a microplate reader every 1 min for 1 h. Measurements were done in duplicate. All duplicate values were averaged and plotted against readout time at 10 min, and the standard error of means was represented as error bars. Note that the inhibitor assays using DPPS-AuNPs follow the same protocol as above except that the absorbance readout time is set at 3 h.

***10.3 Other endogenous mammalian proteins.*** The responsiveness of the sensor to salivary α-amylase, trypsin (Tp), influenza neuraminidase (NA), thrombin (Tb), bovine serum albumin (BSA), and hemoglobin (Hb) was tested. These proteins of desirable amount were spiked into phosphate buffer (10 mM, pH 8.0) to reach a final concentration of 50 nM (*i.e.*, with respect to 120 μL). Note that the final concentration of amylase and neuraminidase is 50 and 5 U/mL, respectively (*i.e.*, with respect to 120 μL). Then, the intact $D_3F_2C_1$ peptide was added, and the assay volume was brought up to 20 μL with phosphate buffer (10 mM, pH 8.0) to reach a final concentration of 100 μM intact peptide (*i.e.*, with respect to 120 μL). Next, the mixtures were tapped, centrifuged, and incubated at 37 °C for 3 h. After that time the assay was transferred into a 96-well plate and incubated with citrate-AuNPs (100 μL, 3.8 nM), and the absorbance at 600 and 520 nm were readout in a microplate reader every 1 min for 1 h. Measurement was done in duplicate. All duplicate values were averaged and plotted against readout time at 10 min, and the standard error of means was represented as error bars. Note that the inhibitor assays using DPPS-AuNPs follow the same protocol as above except for the absorbance readout time at 3 h.

## 11. References

[1] a) L. Zhang, D. Lin, X. Sun, U. Curth, C. Drosten, L. Sauerhering, S. Becker, K. Rox, R.

Hilgenfeld, *Science* **2020**, *368*, 409-412; b) D. M. Mellott, C.-T. Tseng, A. Drelich, P. Fajtová, B. C. Chenna, D. H. Kostomiris, J. Hsu, J. Zhu, A. J. O'Donoghue, J. H. McKerrow, *bioRxiv* **2020**, 2020.2010.2023.347534.
[2] a) Z. Jin, Y. Mantri, M. Retout, Y. Cheng, J. Zhou, A. Jorns, P. Fajtova, W. Yim, C. Moore, M. Xu, M. N. Creyer, R. M. Borum, J. Zhou, Z. Wu, T. He, W. F. Penny, A. J. O'Donoghue, J. V. Jokerst, *Angew. Chem. Int. Ed.* **2022**, *61*, e202112995; b) Z. Jin, J. Yeung, J. Zhou, Y. Cheng, Y. Li, Y. Mantri, T. He, W. Yim, M. Xu, Z. Wu, P. Fajtova, M. N. Creyer, C. Moore, L. Fu, W. F. Penny, A. J. O'Donoghue, J. V. Jokerst, *Chem. Mater.* **2022**, *34*, 1259-1268.
[3] C. Moore, R. M. Borum, Y. Mantri, M. Xu, P. Fajtová, A. J. O'Donoghue, J. V. Jokerst, *ACS Sens.* **2021**, *6*, 2356-2365.
[4] L. Michaelis, M. L. Menten, *Biochem. Z.* **1913**, *49*, 333−369.
[5] V. Henri, *Archivio di Fisiologia* **1904**, *1*, 299-324.
[6] G. E. Briggs, J. B. Haldane, *Biochem J* **1925**, *19*, 338-339.
[7] L. S. Dodda, J. Z. Vilseck, J. Tirado-Rives, W. L. Jorgensen, *J. Phys. Chem. B* **2017**, *121*, 3864-3870.
[8] M. J. Frisch, G. W. Trucks, H. B. Schlegel, G. E. Scuseria, M. A. Robb, J. R. Cheeseman, G. Scalmani, V. Barone, B. Mennucci, D. J. Fox, **2009**.
[9] a) C. A. E. Hauser, R. Deng, A. Mishra, Y. Loo, U. Khoe, F. Zhuang, D. W. Cheong, A. Accardo, M. B. Sullivan, C. Riekel, J. Y. Ying, U. A. Hauser, *Proc. Natl. Acad. Sci. U.S.A.* **2011**, *108*, 1361-1366; b) L. Zhang, Y. Li, G. Mu, L. Yang, C. Ren, Z. Wang, Q. Guo, J. Liu, C. Yang, *Anal. Chem.* **2022**, *94*, 2236-2243.
[10] P. Mark, L. Nilsson, *The Journal of Physical Chemistry A* **2001**, *105*, 9954-9960.
[11] V. Kräutler, W. F. van Gunsteren, P. H. Hünenberger, *Journal of Computational Chemistry* **2001**, *22*, 501-508.
[12] C. Tian, K. Kasavajhala, K. A. A. Belfon, L. Raguette, H. Huang, A. N. Migues, J. Bickel, Y. Wang, J. Pincay, Q. Wu, C. Simmerling, *Journal of Chemical Theory and Computation* **2020**, *16*, 528-552.
[13] H. Bekker, H. J. C. Berendsen, E. J. Dijkstra, S. Achterop, R. Vondrumen, D. Vanderspoel, A. Sijbers, H. Keegstra, M. K. R. Renardus, in *4th International Conference on Computational Physics (PC 92)* (Eds.: R. A. DeGroot, J. Nadrchal), World Scientific Publishing, SINGAPORE, **1993**, pp. 252-256.
[14] M. Schauperl, P. S. Nerenberg, H. Jang, L.-P. Wang, C. I. Bayly, D. L. Mobley, M. K. Gilson, *Communications Chemistry* **2020**, *3*, 44.
[15] T. Lu, F. Chen, *Journal of Computational Chemistry* **2012**, *33*, 580-592.
[16] C. Xue, T. Y. Lin, D. Chang, Z. Guo, *R. Soc. Open Sci.* **2017**, *4*, 160696.
[17] a) M. Di Foggia, P. Taddei, A. Torreggiani, M. Dettin, A. Tinti, *J. Proteome Res.* **2011**, *2*, 231; b) G. Socrates, *Infrared and Raman characteristic group frequencies : tables and charts*, 3rd ed., Wiley, Chichester, England; New York, **2001**.
[18] Z. Jin, L. Du, C. Zhang, Y. Sugiyama, W. Wang, G. Palui, S. Wang, H. Mattoussi, *Bioconjugate Chem.* **2019**, *30*, 871-880.
[19] A. Levin, T. A. Hakala, L. Schnaider, G. J. L. Bernardes, E. Gazit, T. P. J. Knowles, *Nat. Rev. Chem.* **2020**, *4*, 615-634.
[20] D. A. Armbruster, T. Pry, *Clin. Biochem. Rev.* **2008**, *29 Suppl 1*, S49-S52.

# Supplementary Table and Figure

**Table S1.** Molecular weight (M.W.) of the peptide intact (left) and fragment (right).

| Name | Peptide sequence [a] | M. W. (g/mol) | Name | Peptide sequence | M. W. (g/mol) |
|---|---|---|---|---|---|
| $D_3F_0C_1$ | DDDTSAVLQ↓SGDDPC | 1535.6 | C-terminal frag. | SGDDPC | 591.2 |
| $D_3F_1C_1$ | DDDTSAVLQ↓SGGFPC | 1509.6 | C-terminal frag. | SGGFPC | 565.2 |
| $D_3F_2C_1$ | DDDTSAVLQ↓SGFFPC | 1599.7 | C-terminal frag. | SGFFPC | 655.3 |
| $D_3f_2C_1$ | DDDTSAVLQ↓SGPFFC | 1599.7 | N/A | N/A | N/A |
| $D_3F_2C_0$ | DDDTSAVLQ↓SGFFPG | 1553.7 | C-terminal frag. | SGFFPG | 609.3 |
| $D_3F_4C_1$ | DDDTSAVLQ↓SG$(FFP)_2$C | 1990.9 | C-terminal frag. | SG$(FFP)_2$C | 1046.5 |
| $D_3Y_2C_1$ | DDDTSAVLQ↓SGYYPC | 1631.6 | C-terminal frag. | SGYYPC | 687.3 |
| $D_3W_2C_1$ | DDDTSAVLQ↓SGWWPC | 1677.7 | C-terminal frag. | SGWWPC | 733.3 |
| $D_3V_2C_1$ | DDDTSAVLQ↓SGVVPC | 1503.7 | C-terminal frag. | SGVVPC | 559.3 |
| - - | - - | - - | N-terminal frag. (above) | DDDTSAVLQ | 962.4 |
| $S_3F_2C_1$ | SSSTSAVLQ↓SGFFPC | 1515.7 | N-terminal frag. | SSSTSAVLQ | 878.4 |
| $(PAS)_2F_2C_1$ | $(PAS)_2$TSAVLQ↓SGFFPC | 1764.8 | N-terminal frag. | $(PAS)_2$TSAVLQ | 1127.6 |

[a] Peptides have N-terminal $-NH_2$ and amidated C-terminal $-CONH_2$.

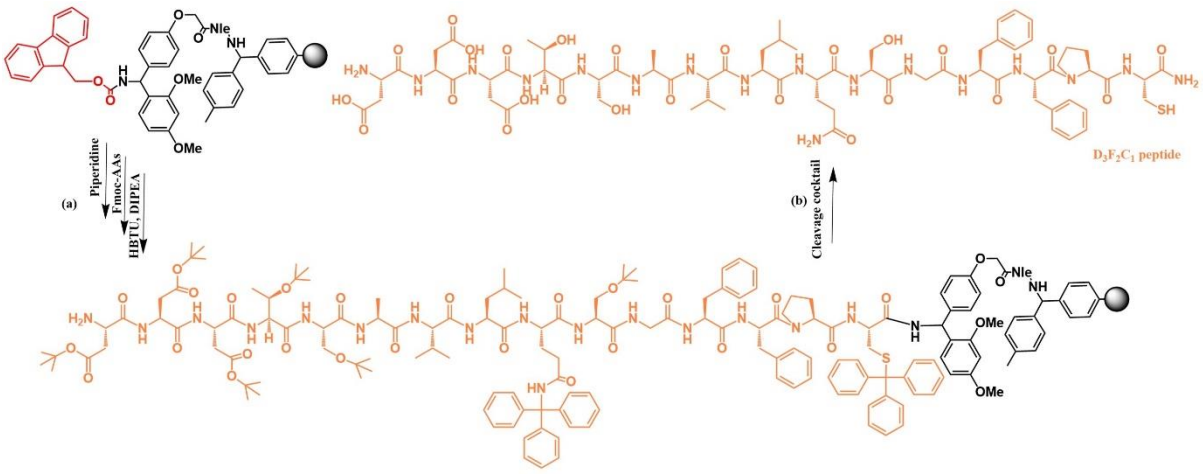


**Figure S1.** The synthetic route of $D_3F_2C_1$ through (**a**) standard solid phase peptide synthesis using Rink-amide-MBHA-resin and (**b**) cocktail cleavage. The ESI-MS of purified peptide is shown in **Figure S2c**.

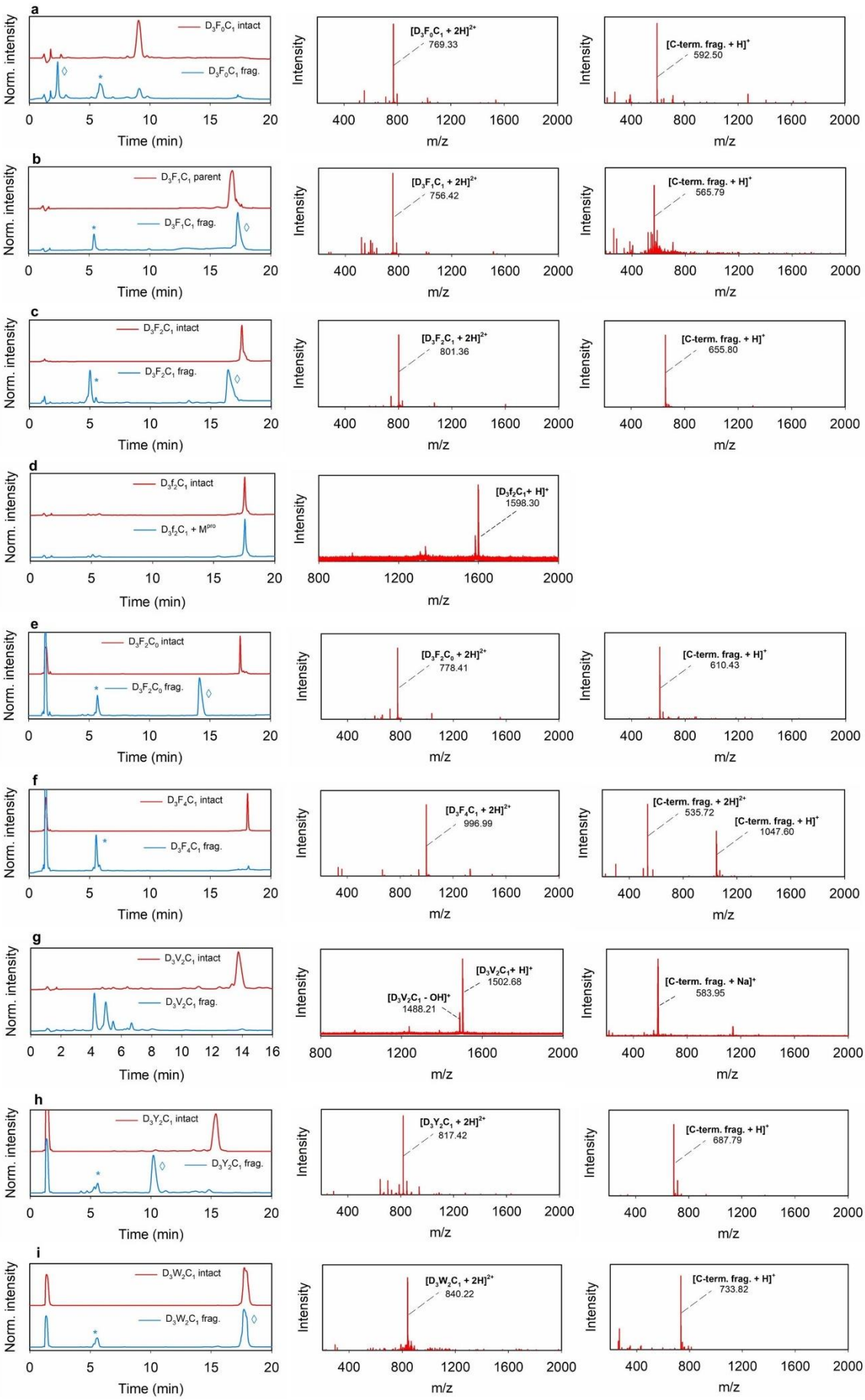
a
Norm. intensity
$D_3F_0C_1$ intact
$D_3F_0C_1$ frag.
Time (min)
Intensity
$[D_3F_0C_1 + 2H]^{2+}$
769.33
m/z
[C-term. frag. + H]$^+$
592.50
b
$D_3F_1C_1$ parent
$D_3F_1C_1$ frag.
$[D_3F_1C_1 + 2H]^{2+}$
756.42
[C-term. frag. + H]$^+$
565.79
c
$D_3F_2C_1$ intact
$D_3F_2C_1$ frag.
$[D_3F_2C_1 + 2H]^{2+}$
801.36
[C-term. frag. + H]$^+$
655.80
d
$D_3f_2C_1$ intact
$D_3f_2C_1$ + M$^{pro}$
$[D_3f_2C_1 + H]^+$
1598.30
e
$D_3F_2C_0$ intact
$D_3F_2C_0$ frag.
$[D_3F_2C_0 + 2H]^{2+}$
778.41
[C-term. frag. + H]$^+$
610.43
f
$D_3F_4C_1$ intact
$D_3F_4C_1$ frag.
$[D_3F_4C_1 + 2H]^{2+}$
996.99
[C-term. frag. + 2H]$^{2+}$
535.72
[C-term. frag. + H]$^+$
1047.60
g
$D_3V_2C_1$ intact
$D_3V_2C_1$ frag.
$[D_3V_2C_1 + H]^+$
1502.68
$[D_3V_2C_1 - OH]^+$
1488.21
[C-term. frag. + Na]$^+$
583.95
h
$D_3Y_2C_1$ intact
$D_3Y_2C_1$ frag.
$[D_3Y_2C_1 + 2H]^{2+}$
817.42
[C-term. frag. + H]$^+$
687.79
i
$D_3W_2C_1$ intact
$D_3W_2C_1$ frag.
$[D_3W_2C_1 + 2H]^{2+}$
840.22
[C-term. frag. + H]$^+$
733.82

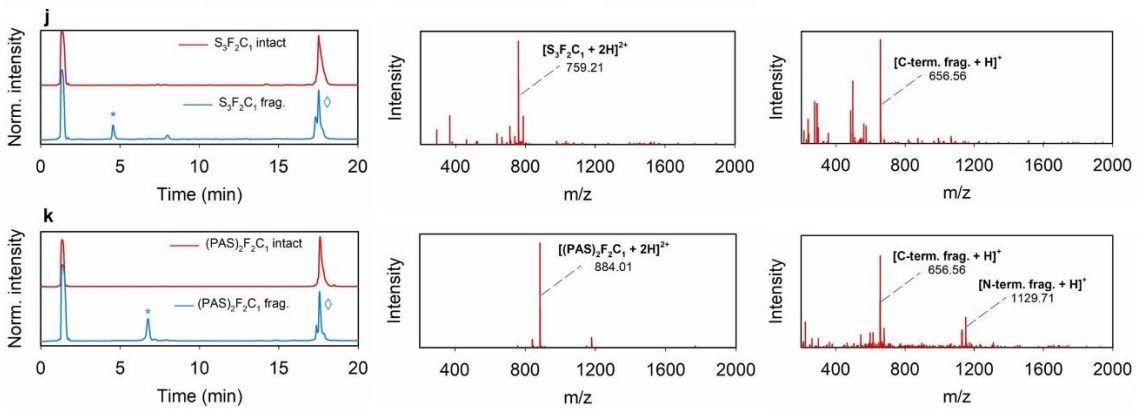


**Figure S2.** HPLC and ESI-MS data of synthetic peptide amphiphiles and the proteolytic products by $M^{pro}$. HPLC is shown in the left panel, and ESI-MS of intact/parent peptide and the corresponding C-terminal fragment (C-term. frag.) are shown in the middle and right panel, respectively. Data collected from the control $D_3F_0C_1$ peptide (**a**), $D_3F_1C_1$ peptide (**b**), $D_3F_2C_1$ peptide (**c**), $D_3f_2C_1$ containing the PFF tripeptide (**d**), non-thiolate $D_3F_2C_0$ peptide (**e**), $D_3F_4C_1$ peptide (**f**), $D_3V_2C_1$ (**g**), $D_3Y_2C_1$ peptide (**h**), $D_3W_2C_1$ peptide (**i**), aprotic-head $S_3F_2C_1$ peptide (**j**), and aprotic-head $(PAS)_2F_2C_1$ peptide (**k**); cleavage occurs after Gln (Q), see **Table 1** for calculated molecular weight. Note that in all HPLC profiles, the strong peak at 1.3 min is the DMSO solvent peak, the "*" label denotes the peak from N-terminal peptide fragment, and the "◊" label represents the peak from C-terminal peptide fragment. Note that $D_3f_2C_1$ peptide has less or no affinity to $M^{pro}$. All the assay condition uses a substrate enzyme ratio of 3000:1, 18 h, 10 mM PB, pH 8.0, and 37 °C.

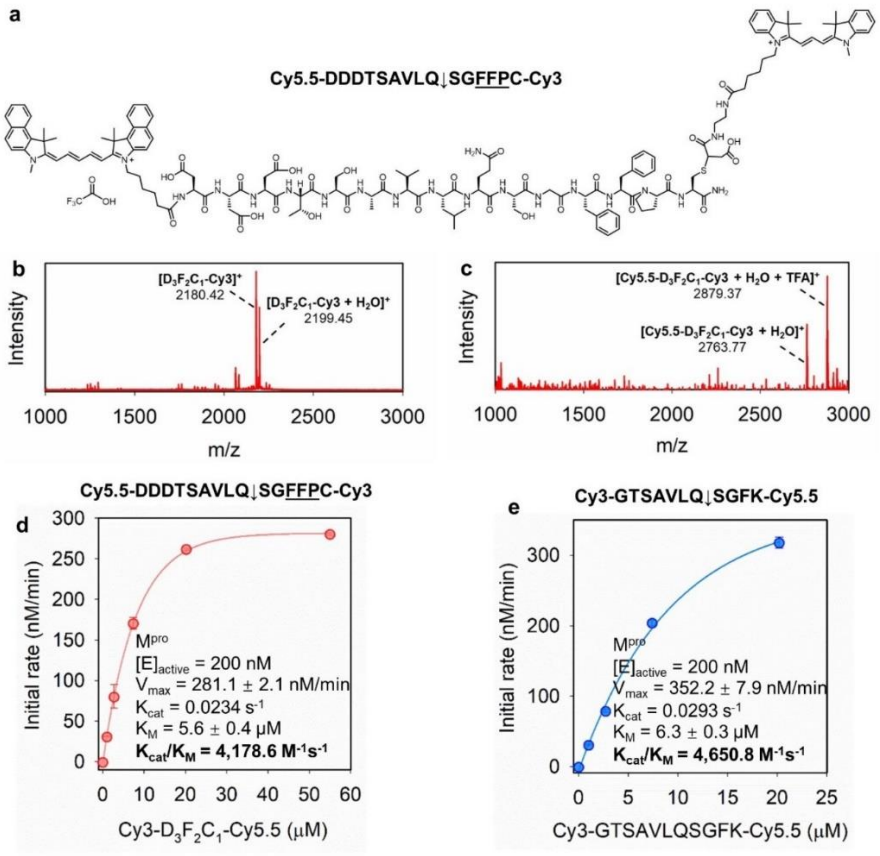


**Figure S3.** Specificity constant ($k_{cat}/K_M$) determination. (**a**) Chemical structure of the as-prepared fluorogenic $D_3F_2C_1$ peptide; the sequence shown is Cy5.5-DDDTSAVLQ↓SGFFPC-Cy3. (**b**) ESI-MS data of DDDTSAVLQ↓SGFFPC-Cy3 via maleimide-cysteine conjugation; 2180.42 m/z was found. (**c**) ESI-MS data of Cy5.5-DDDTSAVLQ↓SGFFPC-Cy3 via NHS-amine conjugation; 2763.77 m/z was found. (**d**) Determination of $K_{cat}$ and $K_M$ for hydrolysis of the $D_3F_2C_1$ by $M^{pro}$ in 10 mM PB, pH 8.0, at 37 °C. The content of DMSO in the assays is < 1% *v/v*. The $M^{pro}$ (active $[E]_0$ = 200 nM) was incubated with the substrate ($[S]_0$ = 0-55 μM) and the concentration of product after 30 min digestion was determined by a standard curve constructed from "ΔPL of Cy3" versus "[DDDTSAVLQSGFFPC-Cy3]". Data were fitted to the Michaelis-Menten equation. (**e**) For comparison, we also show $k_{cat}$ and $K_M$ for hydrolysis of a standard substrate (GTSAVLQ↓SGFK) by $M^{pro}$ under the same conditions.

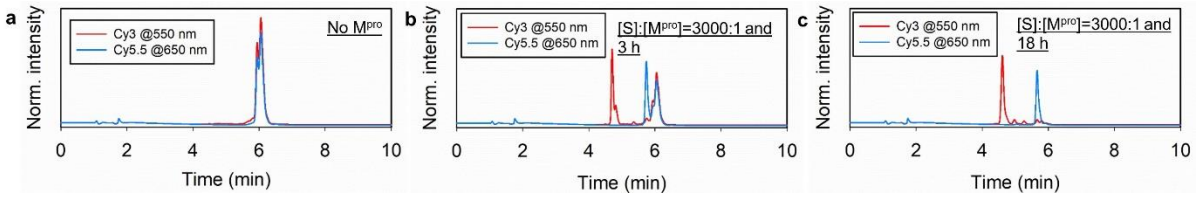


**Figure S4.** HPLC monitoring of the digestion of the $D_3F_2C_1$ SLP by $M^{pro}$ (at a substrate/enzyme ratio of 3000:1) at 3 h (**b**) and 18 h (**b**). The control (**a**) used the pure fluorogenic $D_3F_2C_1$ SLP without $M^{pro}$; The HPLC peak of pure fluorogenic peptide splits because of hydrolysis of the maleimide group. The condition used 10 mM PB, pH 8.0, at 37 °C. The separation of Cy3/Cy5.5 signal indicated complete SLP digestion by $M^{pro}$.

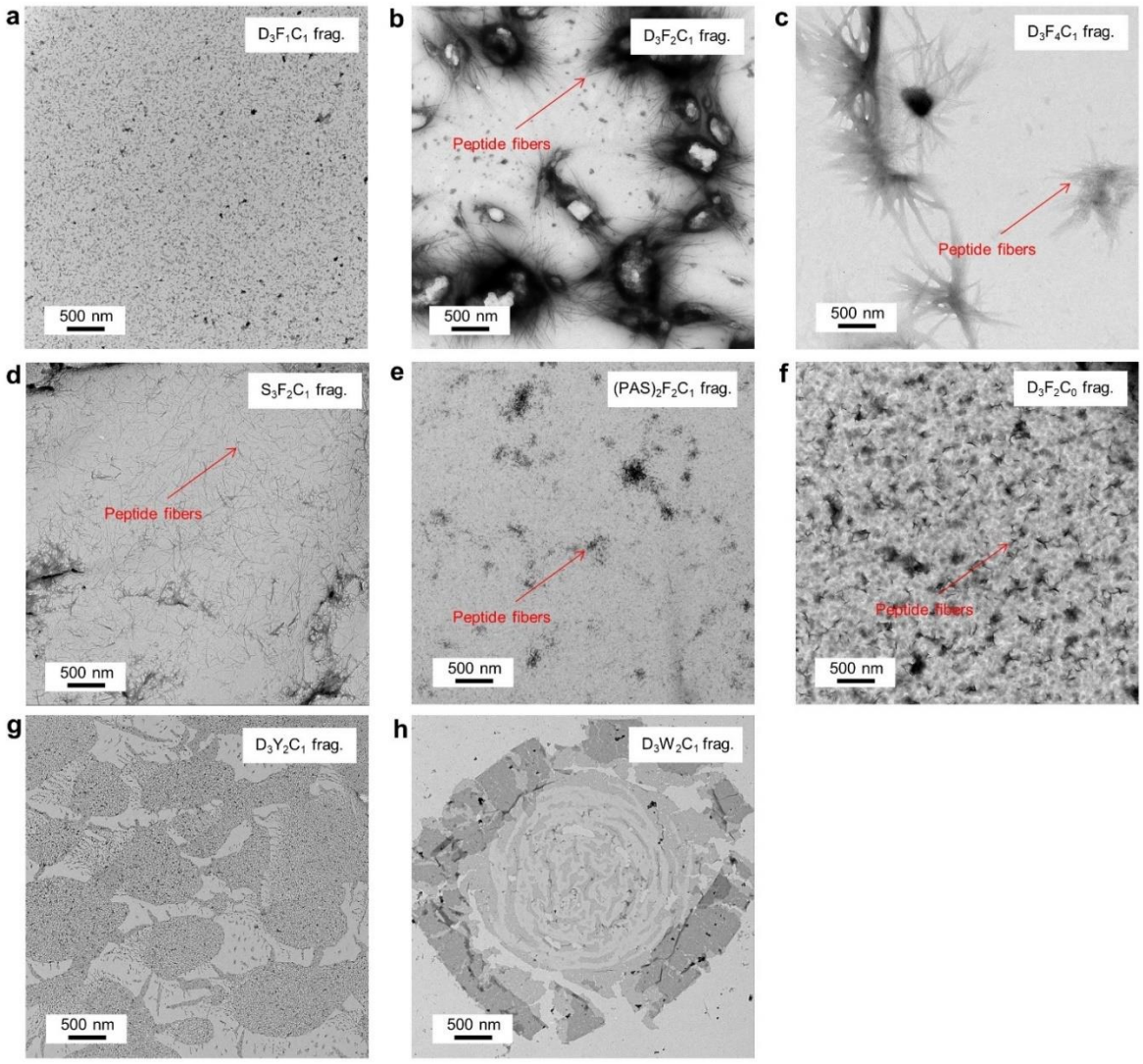


**Figure S5.** TEM zoom-out view of the $M^{pro}$-cleaved products including: $D_3F_1C_1$ peptide (**a**), $D_3F_2C_1$ peptide (**b**), $D_3F_4C_1$ peptide (**c**), aprotic-head $S_3F_2C_1$ peptide (**d**), aprotic-head $(PAS)_2F_2C_1$ fragment (**e**), $D_3F_2C_0$ peptide (**f**), $D_3Y_2C_1$ fragment (**g**), and $D_3W_2C_1$ fragment (**h**). The samples were stained with 0.2% uranyl acetate for TEM imaging. The self-assembled peptide fibers were indicated by the red arrow. The corresponding TEM zoom-in view data were shown in **Figure 1** in the main text. Scale bar = 500 nm.

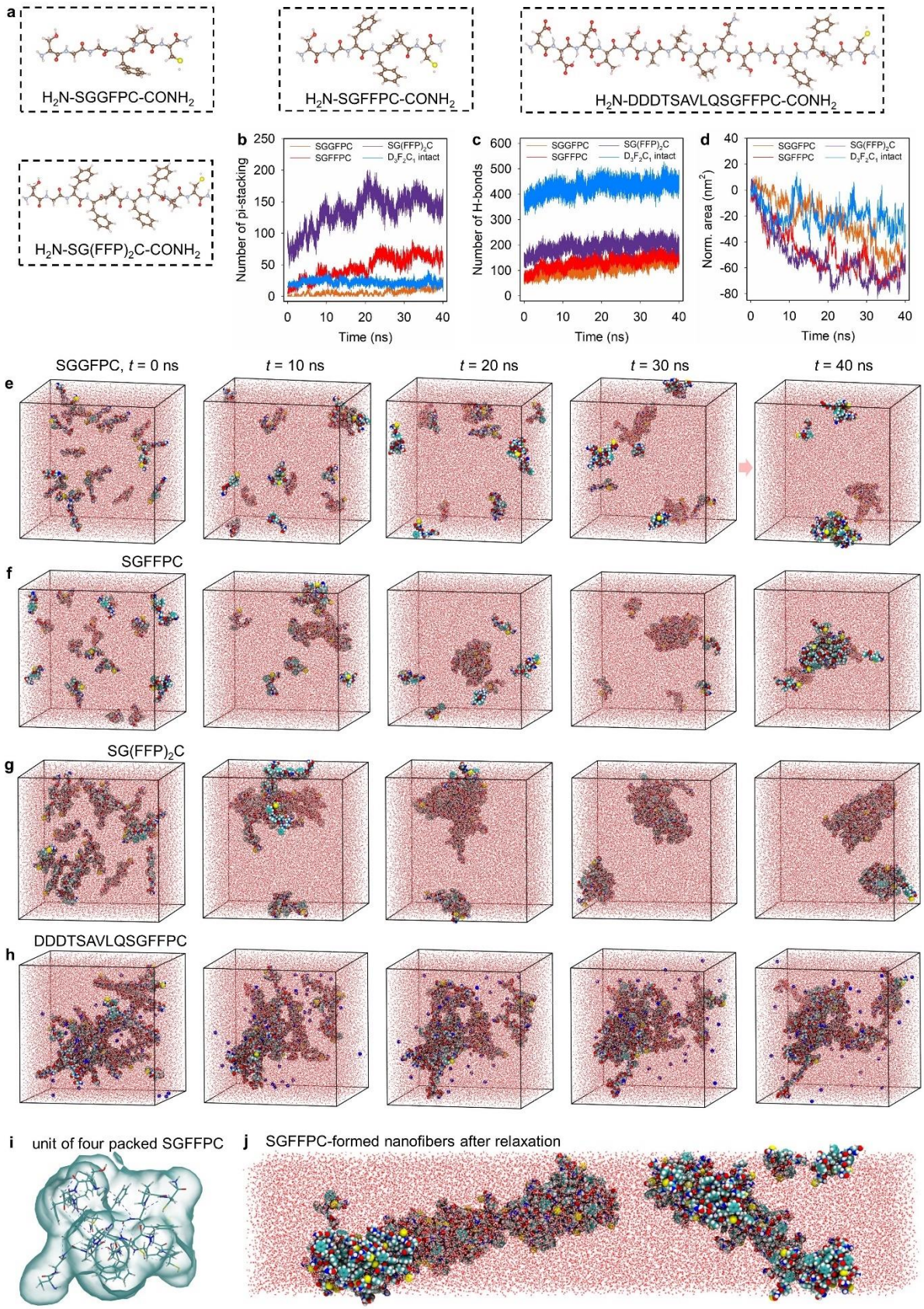


**Figure S6.** Molecular dynamics simulation of peptides in water. (**a**) Chemical structure of four simulated peptides. Structural changes of SGGFPC (**e**), SGFFPC (**f**), SGFFPFFPC (**g**), and DDDTSAVLQSGFFPC (**h**) systems during Gromacs simulation. The snapshots from left to

right were taken at 0, 10, 20, 30, and 40 ns of simulation time. By $t$ = 40 ns, the initial 20 copies of SGFFPC segment assembled to form a peptide aggregate, whereas the $D_3F_2C_1$ peptide (with $Na^+$ counterion) had no clear assembly trend. (**b**) The average value of involved π-stacking interactions at equilibrium for SGGFPC, SGFFPC, $SG(FFP)_2C$, and the intact $D_3F_2C_1$ systems is about 22, 63, 145, and 21, respectively. This indicates that the π-stacking interactions are enhanced by increasing the Phe residue number and are reduced by the $D_3$ stretch. The time-dependent number of hydrogen bonds in above systems was also shown in (**c**). (**d**) The change of solvent-accessible surface area (*i.e.*, $\Delta_{SASA} = SASA_t - SASA_0$) for the above four peptide systems in water are on order of $SG(FFP)_2C \approx$ SGFFPC > SGGFPC > intact $D_3F_2C_1$. (**i**) A cluster of four SGFFPC peptide formed *via* π–π interactions and hydrogen-bonding for simulating the stability of nanofiber structure. (**j**) Final structure from a stacked simulation of an SGFFPC fiber consisting of 64 SGFFPC peptide. After 20 ns of simulation, the constructed fiber remained its tubular structure with slight twisted around the fiber axis.

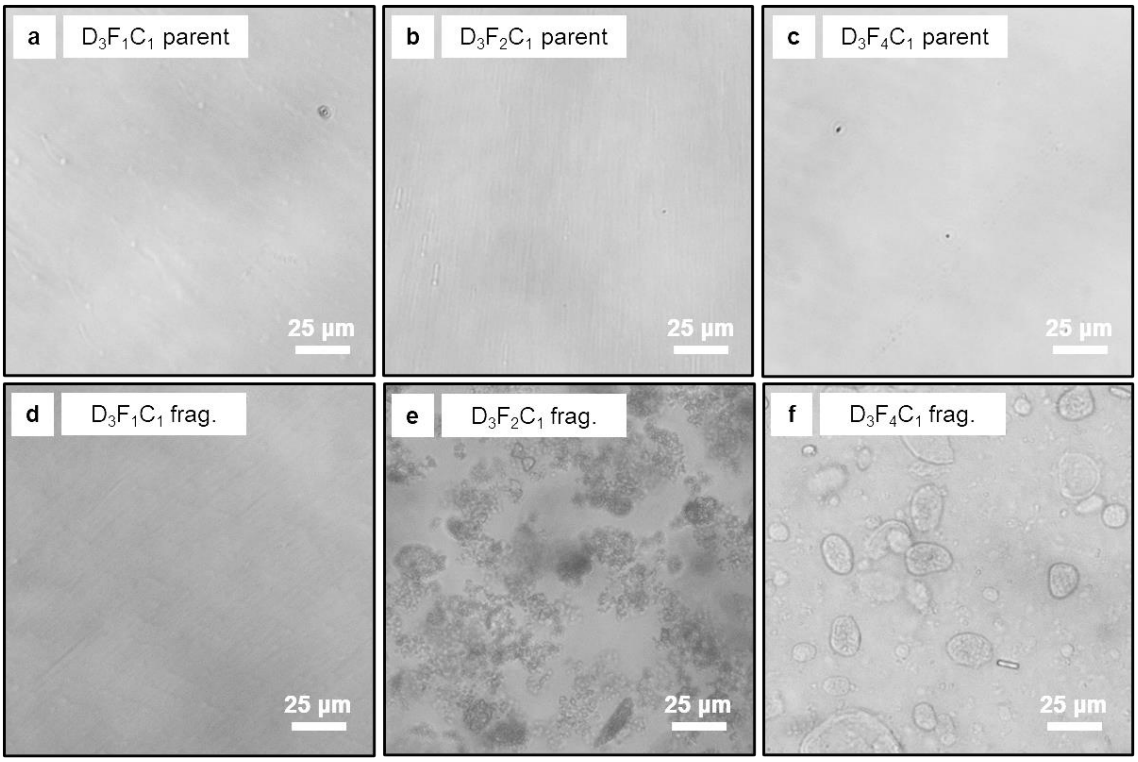


**Figure S7.** Microscopy of the intact/parent peptide solution (1 mg/mL, PB, pH 8.0): $D_3F_1C_1$ (**a**), $D_3F_2C_1$ (**b**), and $D_3F_4C_1$ (**c**). The corresponding solution/suspension treated with $M^{pro}$ containing peptide fragments is shown in panels **d-f**. The $D_3F_2C_1$ fragment (**e**) and $D_3F_4C_1$ fragment (**f**) suspensions showed macroscopic and solid aggregation. Scale bar = 25 μm.

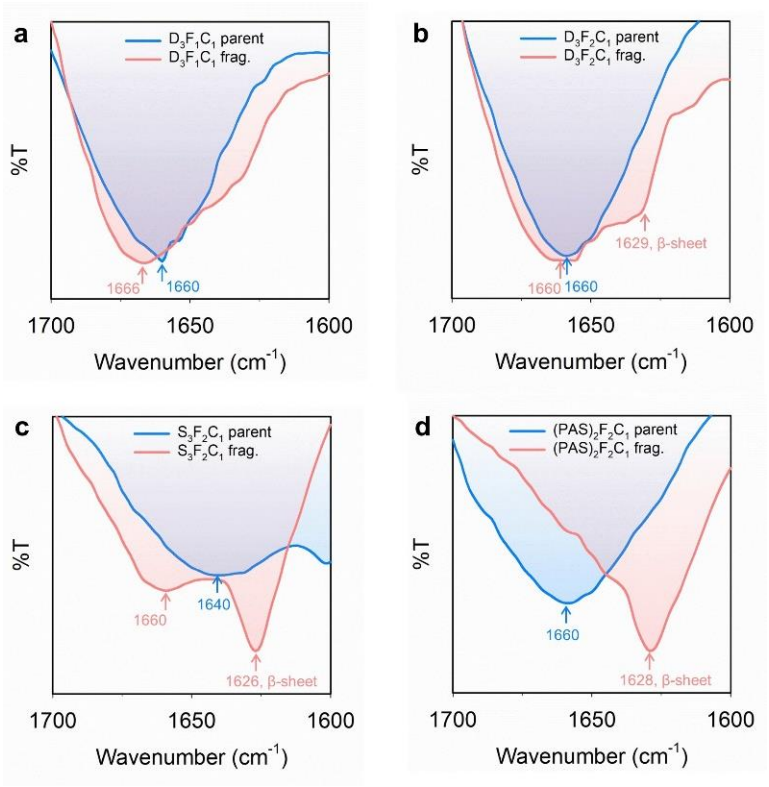


**Figure S8.** FT-IR amide-I region (1700 – 1600 $cm^{-1}$) of $D_3F_1C_1$ (**a**), $D_3F_2C_1$ (**b**), $S_3F_2C_1$ (**c**), and $(PAS)_2F_2C_1$ peptide (**d**). Data profiles from the intact/parent peptide are shown in blue and their corresponding peptide fragments are shown in red. Note that a strong and sharp peak at ~1626 $cm^{-1}$ indicates the predominance of β-sheet secondary structure, while the broad band at ~1660 − 1640 $cm^{-1}$ denotes the presence of amide bond (*i.e.*, C=O stretching).[17a] The assembled β-sheet visually presents in $F_2C_1$ suspensions but not $F_1C_1$ fragment. More data interpretation is provided in the **Section 6**, **Supplementary Information**.

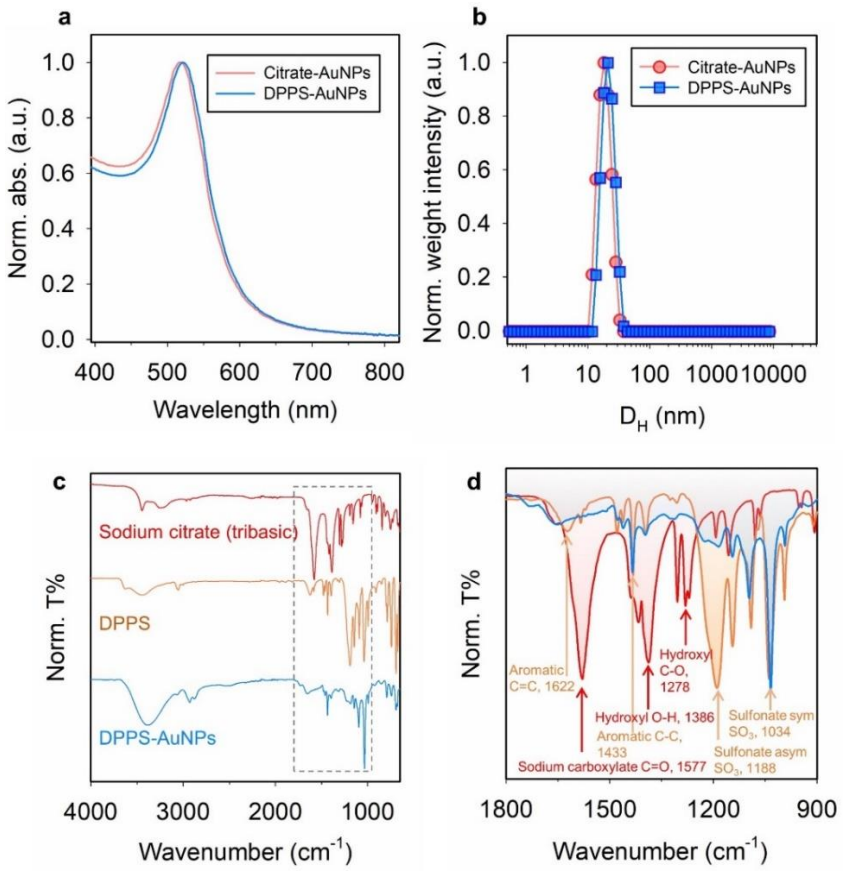


**Figure S9.** Characterization of gold colloids. (a) Optical absorption profiles of citrate-AuNPs (SPR ~518 nm, red) and DPPS-AuNPs (SPR ~521 nm, blue). A slight increase of the maximum absorbance of the SPR band from 518 to 521 nm is attributed to changes of the dielectric environment around nanoparticles due to the new ligand. (b) DLS profiles of citrate-capped AuNPs ($D_H$ = 18.2 nm, PDI=0.09, red) and DPPS-coated AuNPs ($D_H$ = 21.0 nm, PDI= 0.15, blue). Panel (**c**) shows the FT-IR spectra over the range 4000−650 $cm^{-1}$ collected from the native sodium citrate tribasic (red); native DPPS chemical (yellow); and DPPS-AuNP pellet prepared *via* DPPS ligand exchange over citrate-AuNPs (blue). The dashed box indicates the signature peaks of both surface ligands. Panel (**d**) shows a close-up of those spectra over range 1800−900 $cm^{-1}$, where the C=O signatures are associated with the carboxylates in sodium citrate (red), and S−O signatures are from DPPS (yellow and blue). This indicates a successful ligand exchange to make the DPPS-AuNPs. See TEM characterization of the colloidal gold in **Figure S10**.

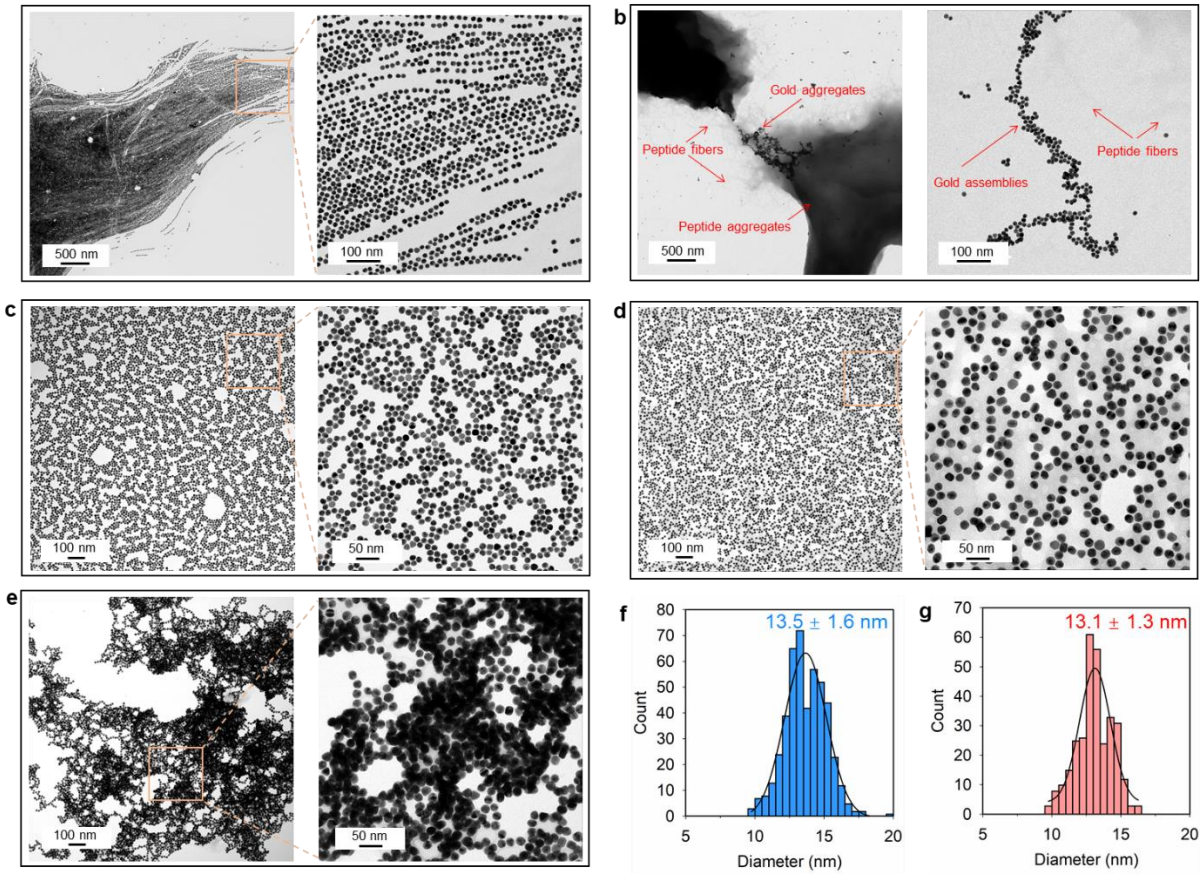


**Figure S10.** TEM imaging (left: zoom-out, right: zoom-in view) of citrate-AuNPs in the presence of intact $D_3F_2C_1$ peptide (**a**) and $D_3F_2C_1$ fragments (**b**). In panel (**b**), the gold nanoparticles cluster into random chains near peptide-fragment assemblies due to the sulfhydryl-rich and aromatic zipper properties. Panel (**c**) shows the mono-dispersed DPPS-AuNPs only in water. TEM imaging of DPPS-AuNPs in the presence of intact $D_3F_2C_1$ peptide (**d**) and $D_3F_2C_1$ fragments (**e**). A histogram of particle size extracted from the TEM images, with an average diameter of $d$ = 13.5 ± 1.6 nm for citrate-AuNPs (**f**) and $d$ = 13.1 ± 1.3 nm for DPPS-AuNPs (**g**). Size distribution was analyzed in ImageJ by counting more than 300 particles using a manual method.

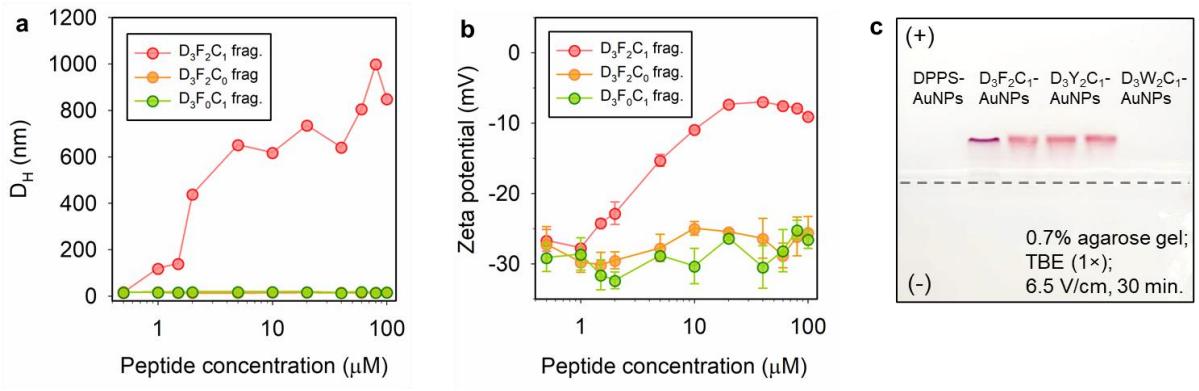


**Figure S11.** (**a**) DLS profiles of citrate-AuNPs (3.4 nM, 100 μL) incubated with increasing concentrations of $D_3F_2C_1$ fragment (red), $D_3F_2C_0$ fragment (yellow), and $D_3F_0C_1$ fragment (green). No change of the hydrodynamic diameter ($D_H$) for citrate-AuNPs was observed when incubated with peptide fragments lacking Phe (F) or Cys (C), while such a change became sizable in the presence of $F_2C_1$ fragment of more than ~1 μM. (**b**) Zeta potential measurements of citrate-AuNPs (3.4 nM, 100 μL) incubated with increasing concentrations of $D_3F_2C_1$ fragment (red), $D_3F_2C_0$ fragment (yellow), and $D_3F_0C_1$ fragment (green). The $D_3F_2C_1$ fragment (*i.e.*, SGFFPC) displaced the surface citrate molecules and altered the surface charges from −29.5 to −6.5 mV. While $D_3F_0C_1$ fragment (*i.e.*, SGDDPC) displaced the surface citrate and compensated the surface potential with two aspartates, thus essentially no potential change. The $D_3F_2C_0$ fragment (*i.e.*, SGFFPG) has no interaction with gold surfaces due to the lack of cysteine anchor thus no change on the zeta potential. Error bars represent triplicate measurements for one sample. (**c**) Agarose gel electrophoresis images collected from DPPS-AuNPs only and DPPS-AuNPs incubated with intact $D_3F_2C_1$, $D_3Y_2C_1$, and $D_3W_2C_1$ peptide. Gel conditions are given on the bottom right, and the samples were prepared using a mixture of 10 μL glycerol and 40 μL AuNPs (~8 nM). Note that TBE buffer (1×) could promote slight aggregation of DPPS-AuNPs after 30 min.

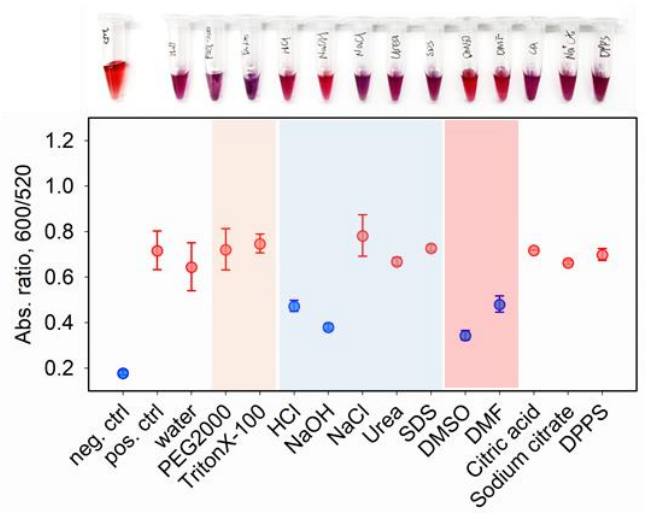


**Figure S12.** Probing interparticle interactions. (Top) A white-light image of aggregated nanoparticles (by $D_3W_2C_1$ fragment, *i.e.*, SGWWPC) redispersed in different media (from left to right: citrate-AuNP dispersion control, water, $PEG_{2000}$, TritonX-100, HCl, NaOH, NaCl, urea, SDS, DMSO, DMF, citric acid, sodium citrate, and DPPS). The solutions were at 10 mM except for urea at 1 M. (Bottom) Ratiometric absorption quantification of the imaging. Blue data points indicate dispersed nanoparticles while the red data points indicate aggregated nanoparticles. The error bars represent standard deviations (n = 2). The dominant interactions in $W_2C_1$-aggregated nanoparticles were aromatic π–π stacking (*i.e.*, can redisperse in DMSO/DMF) and hydrogen bonding (*i.e.*, can redisperse in HCl/NaOH solution).

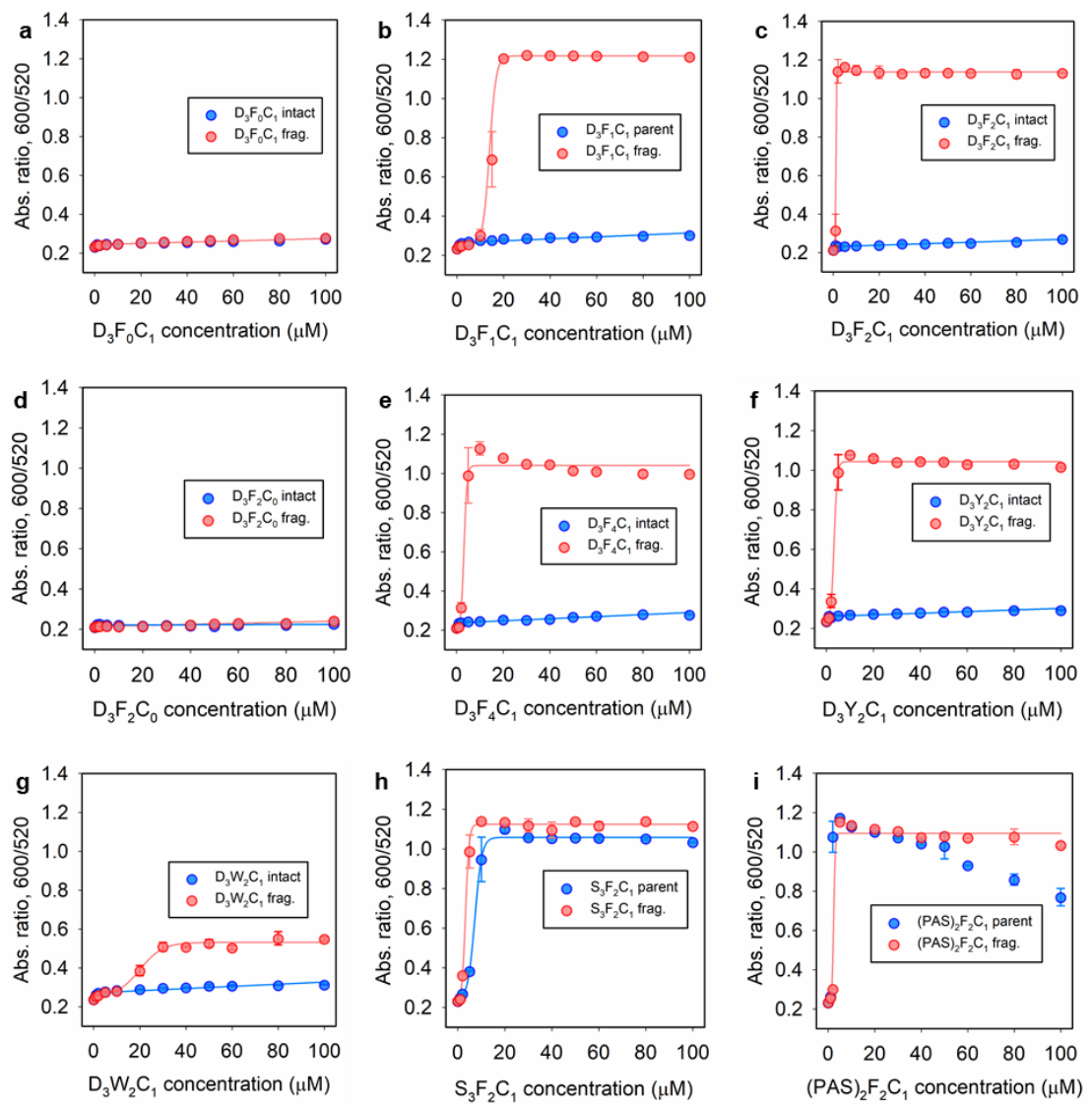


**Figure S13.** Operation window of different sensing peptides for $M^{pro}$ using citrate-AuNPs. Ratiometric signal ($Abs_{600}/Abs_{520}$) collected from citrate-AuNPs (3.4 nM, 100 μL) incubated with various amount of intact/parent peptide (blue) and fragments (red), including $D_3F_0C_1$ peptide (**a**), $D_3F_1C_1$ peptide (**b**), $D_3F_2C_1$ peptide (**c**), $D_3F_2C_0$ peptide (**d**), $D_3F_4C_1$ peptide (**e**), $D_3Y_2C_1$ peptide (**f**), $D_3W_2C_1$ peptide (**g**), aprotic-head $S_3F_2C_1$ peptide (**h**), and aprotic-head $(PAS)_2F_2C_1$ peptide (**i**).

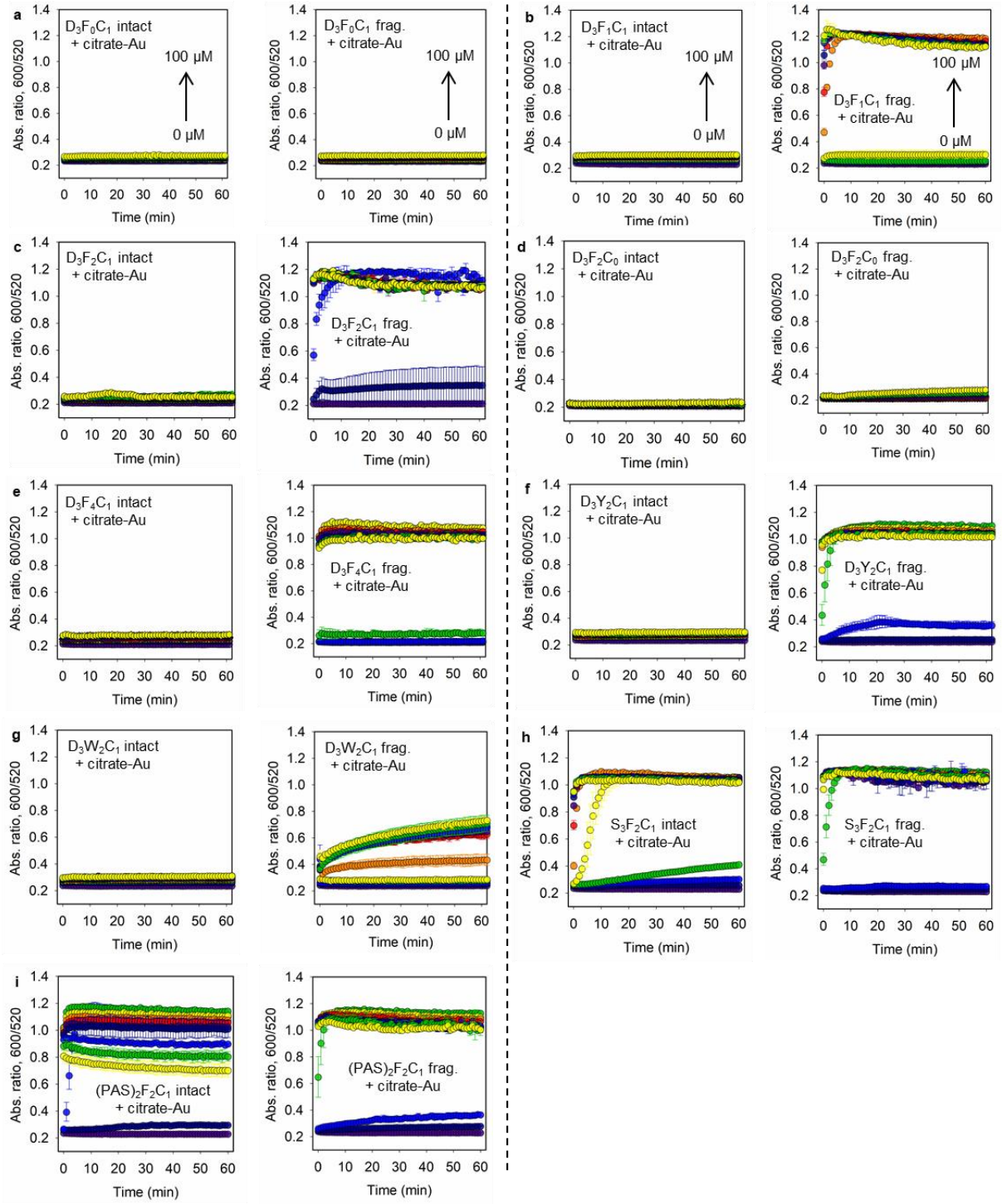


**Figure S14.** Time progression of ratiometric absorbance ($Abs_{600}/Abs_{520}$)**,** where citrate-AuNPs (3.4 nM, 100 μL) are incubated with increasing concentrations of the intact/parent peptide (left panel) or its proteolytic fragments (right panel, 0−100 μM), including $D_3F_0C_1$ peptide (**a**), $D_3F_1C_1$ peptide (**b**), $D_3F_2C_1$ peptide (**c**), $D_3F_2C_0$ peptide (**d**), $D_3F_4C_1$ peptide (**e**), $D_3Y_2C_1$ peptide (**f**), $D_3W_2C_1$ peptide (**g**), aprotic-head $S_3F_2C_1$ peptide (**h**), and aprotic-head $(PAS)_2F_2C_1$ peptide (**i**). Phosphate buffer (10 mM, pH 8.0) was used, and the readout time is set at 10 min. Error bar = standard deviation (n = 2). The extracted operation window for each peptide is provided in **Figure S13**.

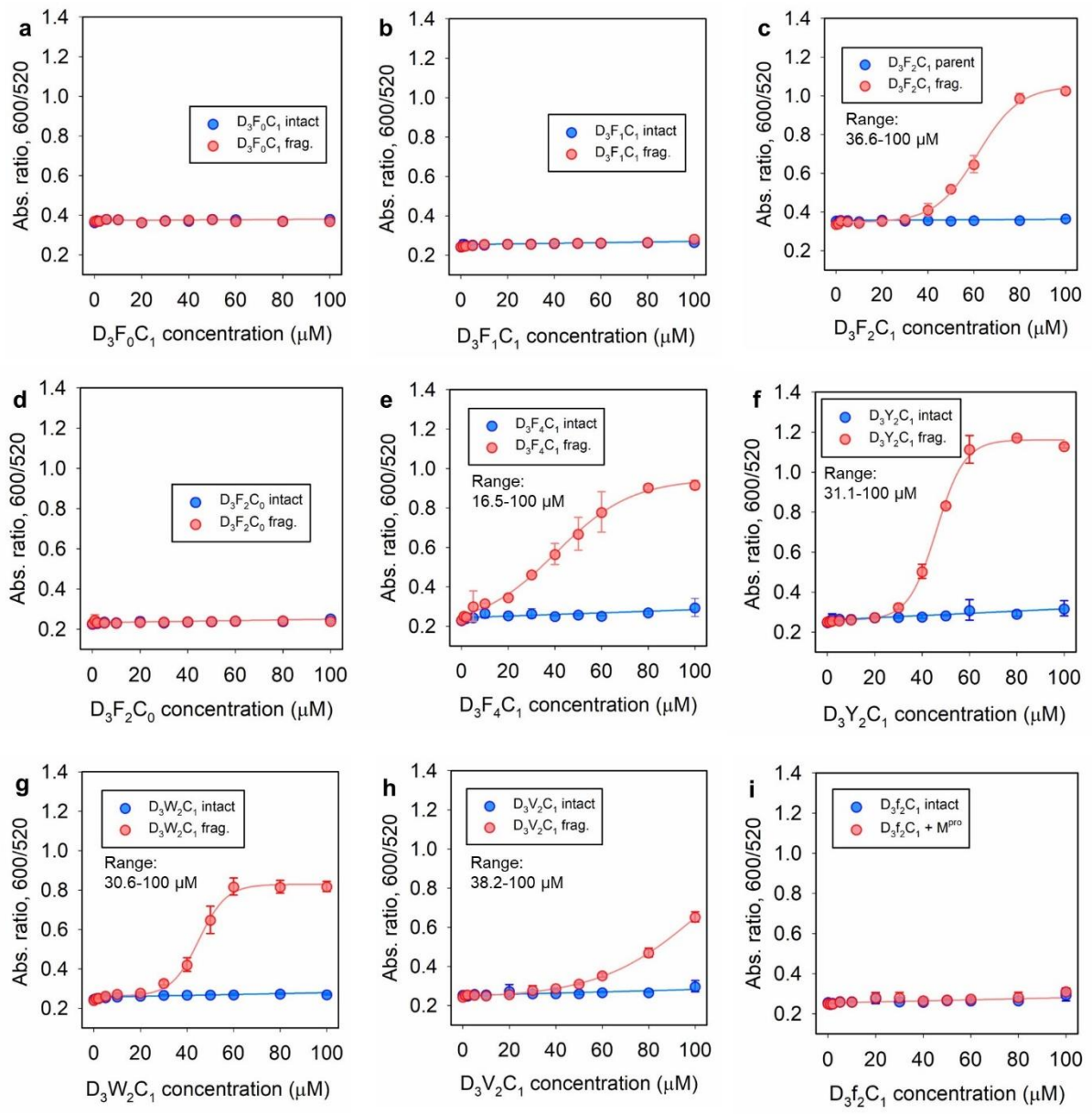


**Figure S15.** Operation window of different sensing peptides for $M^{pro}$ using DPPS-AuNPs. Ratiometric signal ($Abs_{600}/Abs_{520}$) collected from DPPS-AuNPs (3.4 nM, 100 μL) incubated with various amount of intact/parent peptide (blue) and fragments (red), including $D_3F_0C_1$ peptide (**a**), $D_3F_1C_1$ peptide (**b**), $D_3F_2C_1$ peptide (**c**), $D_3F_2C_0$ peptide (**d**), $D_3F_4C_1$ peptide (**e**), $D_3Y_2C_1$ peptide (**f**), $D_3W_2C_1$ peptide (**g**), $D_3V_2C_1$ peptide (**h**), and $D_3f_2C_1$ peptide (**i**). The extracted operation window for all peptides was also provided.

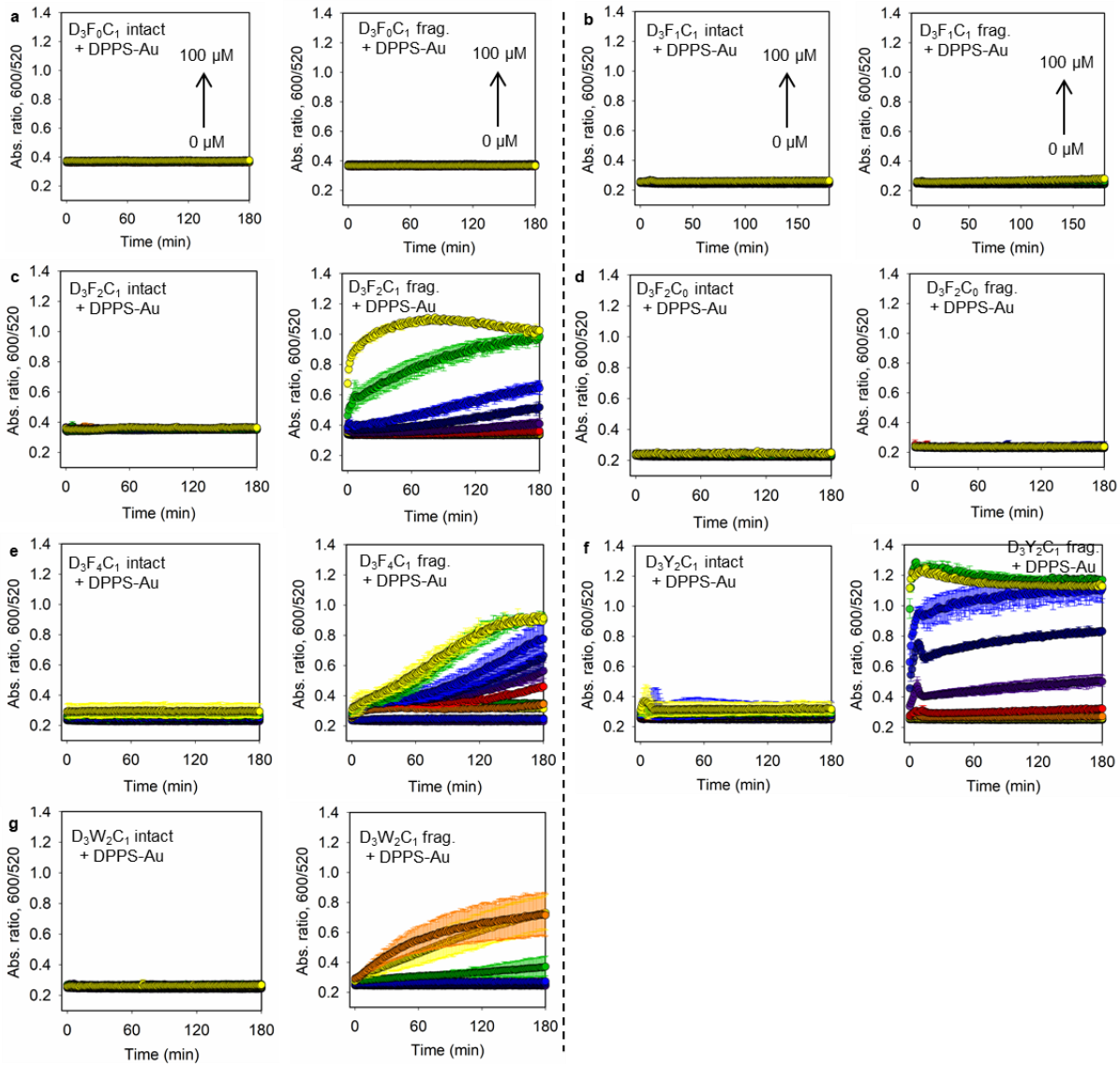


**Figure S16.** Time progression of ratiometric absorbance ($Abs_{600}/Abs_{520}$)**,** where DPPS-AuNPs (3.4 nM, 100 μL) are incubated with increasing concentrations of the intact/parent peptide (left panel) or its proteolytic fragments (right panel, 0−100 μM), including $D_3F_0C_1$ peptide (**a**), $D_3F_1C_1$ peptide (**b**), $D_3F_2C_1$ peptide (**c**), $D_3F_2C_0$ peptide (**d**), $D_3F_4C_1$ peptide (**e**), $D_3Y_2C_1$ peptide (**f**), and $D_3W_2C_1$ peptide (**g**). Phosphate buffer (10 mM, pH 8.0) was used, and the readout time is set at 10 min. Error bar = standard deviation (n = 2). The extracted operation window for each peptide is shown in **Figure S15**.

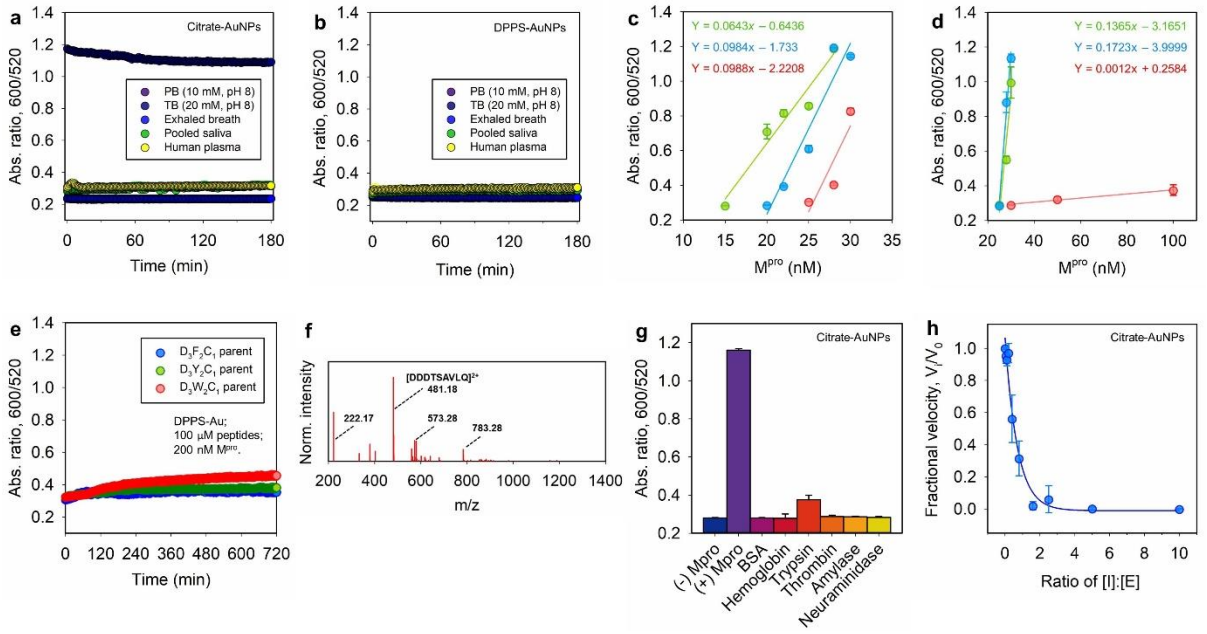


**Figure S17.** (**a**) Ratiometric absorption test shows that citrate-AuNPs were stable in PB buffer (10 mM, pH 8.0), exhaled breath condensate (EBC), 50% diluted pooled saliva (from LeeBio, Inc.), and 50% diluted human plasma for at least 3 h. Note that high ionic strength TB buffer (*e.g.*, 20 mM, pH 8.0) aggregated the citrate-AuNPs. (**b**) DPPS-AuNPs were stable in all tested media for at least 3 h. The linear regions used to calculate LoDs in different media (green: PB buffer, blue: EBC, and red: saliva) when using citrate-AuNPs (**c**) and DPPS-AuNPs (**d**). The best fitting functions were given and the extracted LoDs were shown in **Figure 5** in the main text. (**e**) One-pot protease assays showed no signal activation, where the intact $D_3F_2C_1$/ $D_3Y_2C_1$/ $D_3W_2C_1$ peptide (100 μM)-mixed DPPS-AuNPs (3.4 nM, 100 μL) were incubated with a fixed amount of $M^{pro}$ (200 nM) at 37 °C for 6 h. This is due to the peptide on the space-limited nanosurfaces cannot be accessed by the soluble $M^{pro}$. (**f**) ESI-MS of the supernatant collected from the reaction of $D_3F_2C_1$-AuNPs with $M^{pro}$ (by centrifuge). The peak at 481.18 m/z is assigned to the $M^{pro}$-cleaved $D_3F_2C_1$ fragment (C-terminal), which is from the proteolytic product of the surface-uncoordinated peptide. (**g**) $D_3F_2C_1$/citrate-AuNPs-based sensor responsiveness by other mammalian proteins (50 nM), including bovine serum albumin (BSA), hemoglobin, trypsin, thrombin, α-amylase (50 U/mL), and neuraminidase (5 U/mL). Samples with and without $M^{pro}$ were the positive and negative control. (**h**) Typical inhibition titration curve with a guideline collected by using GC376 chemical. The combination of $D_3F_2C_1$ peptide and citrate-AuNPs were used. Error bar = standard deviation (n = 2).